A RECONNAISSANCE INVESTIGATION OF CHALCOPYRITE-SPHALERITE RELATIONSHIPS IN THE Cu-Fe-Zn-S SYSTEM

by

Lovell B. Wiggins

Thesis submitted to the Graduate Faculty of the
Virginia Polytechnic Institute and State University
in partial fulfillment of the requirements for the degree of
MASTER OF SCIENCE
in
Geological Sciences

APPROVED:

J. R. Craig, Chairman

P. H. Ribbe

M. C. Gilbert

August, 1974

Blacksburg, Virginia

ACKNOWLEDGMENTS

I wish to express my appreciation to the members of my graduate committee for their advice and encouragement, Dr. P. H. Ribbe, Dr. D. A. Hewitt and Dr. M. C. Gilbert. Dr. J. R. Craig, as chairman, shared my enthusiasm for the topic as both a teacher and a friend.

Without the assistance of the American and Canadian Mines listed below, who so generously supplied samples for the research effort, the thesis would have been sadly lacking. I am extremely grateful for their consideration.

Brunswick Tin Mines Ltd.
Sherritt Gordon Mines Ltd.
Sullivan Mining Group Ltd.
Anaconda Britannia Mines
American Smelting and Refining Company
Long Lac Mineral Exploration Limited
Heath Steele Mines Limited
Hudson Bay Mining and Smelting Co., Ltd.
Brunswick Mining and Smelting Corp., Ltd.

TABLE OF CONTENTS

LIST OF TABLES

LIST OF FIGURES

INTRODUCTION

The Cu-Fe-Zn-S system (Figure 1) embraces the largest and most common family of sulfide minerals. Included are the major primary sources of copper and zinc, the minerals chalcopyrite and sphalerite, respectively. The more common of the phases in this system (pyrite, pyrrhotite, chalcopyrite, and sphalerite) frequently occur together, forming the copper-zinc ores. Frequently sphalerite and chalcopyrite and sometimes sphalerite and pyrrhotite are intimately intergrown displaying textures which have been variously interpreted as the products of exsolution or replacement. Minerals from this system have been found in all rock types ranging from meteoritic to sedimentary and have been considered as forming by such diverse mechanisms as aqueous low temperature chemical precipitation and magmatic differentiation. These minerals are especially prevalent, however, in ores of hydrothermal origin.

The purpose of this investigation is to provide insight into the phase relations of the Cu-Fe-Zn-S quarternary system between 800°C and 500°C. Predominant emphasis is placed on the sphalerite-chalcopyrite relationships within the pyrite, pyrrhotite, sphalerite, chalcopyrite and cubanite portion of the system correlative with typical copper-zinc ores. Interest in the relationships between chalcopyrite and sphalerite arises from their common mutual occurrence as constituents of the major Cu-Zn ores. The approach to elucidation of the relationships between chalcopyrite and sphalerite has two aspects: (1) experimental investigation of synthetic Cu-Fe-Zn-S

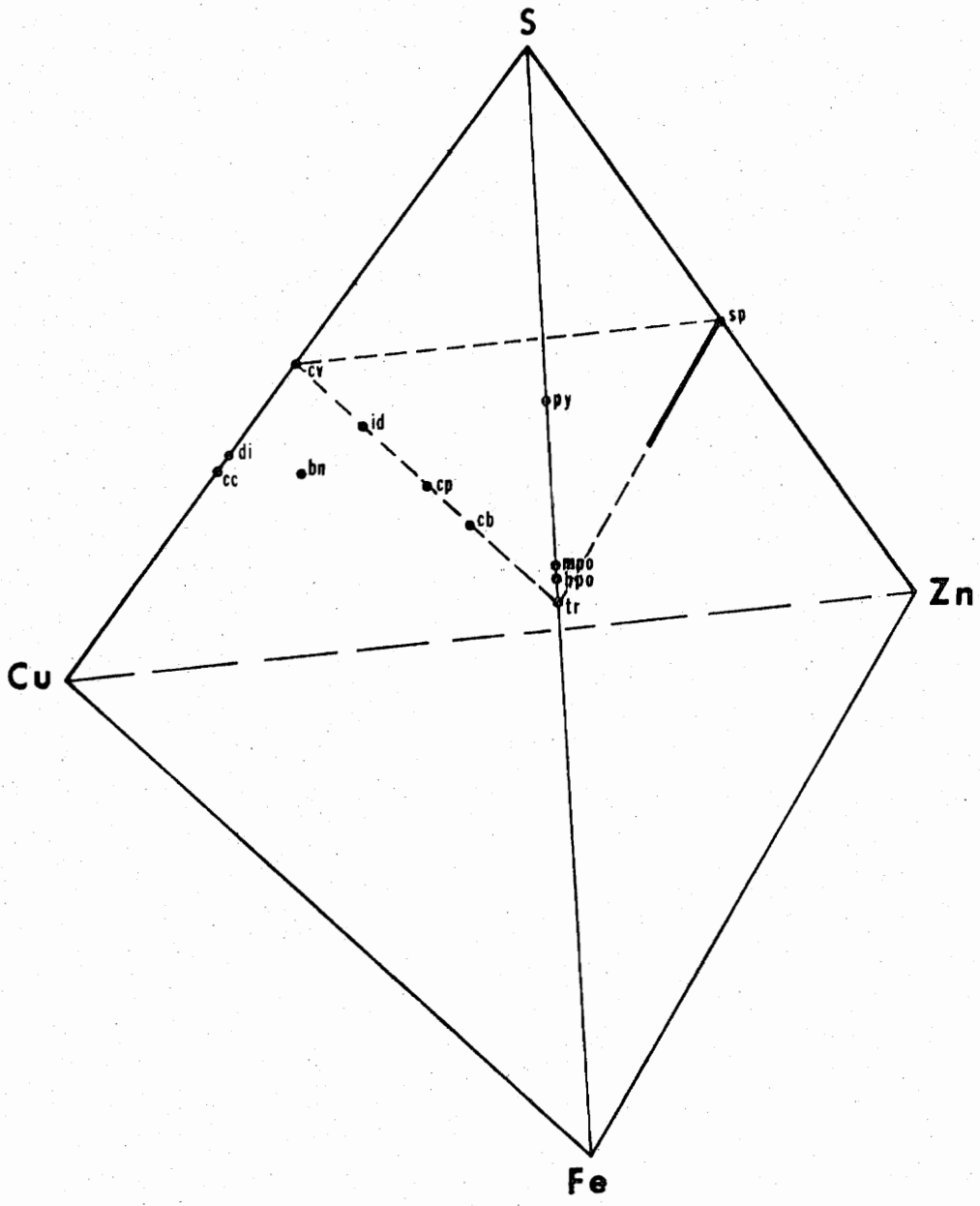

Figure 1. Schematic Representation of the Phases of Primary Interest. Abbreviations are tr-troilitte, hpo-hexagonal pyrrhotite, mpo-monoclinic pyrrhotite, py-pyrite, sp-sphalerite, cv-covellite, di-digenite, cc-chalcocite, bn-bornite, id-idaite, cp-chalcopyrite, cb-cubanite.

assemblages, and (2) examination of natural assemblages containing chalcopyrite and sphalerite. The large temperature gap between 500°C, the lowest temperature of study, and the temperatures at which the ores equilibrated obviously makes correlation of the present experimental work with natural ore occurrences very speculative. However, this study is intended only as a reconnaissance of the system and represents the first steps into an extremely complex mineral system. It is hoped the present study will serve as a foundation for more detailed studies over the same temperature range and as a guide to additional investigations at lower temperatures.

PREVIOUS WORK

The experimental investigation is necessarily built upon a fundamental knowledge of the Cu-Fe-S, Zn-Fe-S, and Cu-Zn-S ternaries. The results of these ternary studies are as follows:

Cu-Fe-S. The historic and precedent-setting research by Merwin and Lombard (1936) which delineated the major phase fields and demonstrated the obvious importance and complexity of the system's phase relations prompted a multitude of detailed studies dealing with selected portions of the ternary (for a complete listing see Cabri, 1973). The latest works to treat the Cu-Fe-S ternary as a unit were that of Yund and Kullerud (1966) and Kullerud et al. (1969). In addition there was a multi-segment study by Barton (1973), the first part of which covered the Cu-S and Cu-Fe-S joins.

The works of previous researchers outlined the phase relationships of the copper and iron sulfides considered in this study, i.e., covellite, pyrrhotite, cubanite, bornite, chalcopyrite, idaite, and the intermediate solid solution (iss). The thermal stabilities of these phases are listed in Table 1 and their phase relationships are summarized in Figure 2. It is of particular importance to note the three phases exhibiting solid solution: pyrrhotite, high digenite-bornite, and iss.

Zn-Fe-S. The first important study involving this system was conducted along the FeS-ZnS join by Kullerud (1953) and produced the "sphalerite-pyrrhotite geothermometer." Subsequent work in this same area was performed by Barton and Kullerud (1957) and by Skinner et al. (1959). The first treatment of the system as a ternary appeared in papers by Barton and Toulmin (1963, 1964); these works negated the "sphalerite-pyrrhotite geothermometer." Such studies demonstrated that the solubility of FeS in ZnS, in the presence of iron, is 56 mol percent at 850°C. Because this solid solubility is rather insensitive to temperature changes, it is of little value as a geothermometer. They also found that in the presence of pyrite solid solubility of FeS in ZnS is only 13 mol percent at 745°C. These relationships are outlined in Figure 3.

Cu-Zn-S. This system has been investigated by Fredrick (1908), Novaselov (1955), Nesterov and Ponomareo (1958, 1960), Moh (1960), and Craig and Kullerud (1973). Craig and Kullerud (1973) examined the phase relationships through the range 100°C to 1050°C with

Table 1

Phase	Abbreviations	Stoichoimetric Composition	Crystallography and References	Thermal Stability T, °C and References
Covellite	cv	CuS	hexagonal	to 507 (1)(5)
Pyrrhotite	po	$Fe_{1-x}S$	hexagonal**(12)	>90 (2)
Pyrite	py	FeS_2	cubic	to 743 (3)
Bornite	bn	Cu_5FeS_4	cubic (13)	>228 (4)(5)
Idiaite	id	Cu_3FeS_4	hexagonal (14)	to 501 (5)
Chalcopyrite	cp	$CuFeS_2$	tetragonal (7)	to 547±5 (7), to 557 (6)*
Cubanite	cb	$CuFe_2S_3$	cubic	252 (7)*
Sphalerite	sp	ZnS	cubic	pure ZnS to 1,020 (8) with 56% FeS to between 850 and 875 (9)
Chalcocite	cc	Cu_2S	cubic (15)	425±20 to 1105 (10)
Intermediate Solid Solution	iss	wide range	cubic (11)	depends on composition, lowest between 20 and 200 (11)

References:

(1) Kullerud (1958); (2) Kissin (1974); (3) Kullerud and Yoder (1959); (4) Yund and Kullerud (1961); (5) Roseboom and Kullerud (1958); (6) Pankrantz and King (1970; (7) Yund and Kullerud (1966); (8) Allen and Crenshaw (1912); (9) Barton and Toulmin (1966); (10) Jensen (1947); (11) Cabri (1973); (12) Carpenter and Desborough (1964); (13) Morimoto (1964); (14) Yund (1963); (15) Kullerud and Yund (1960).

* Phases that compose the intermediate solid solution in their cubic form.

** The pyrrhotites encountered in this study are hexagonal and of the nickel arsenide structure.

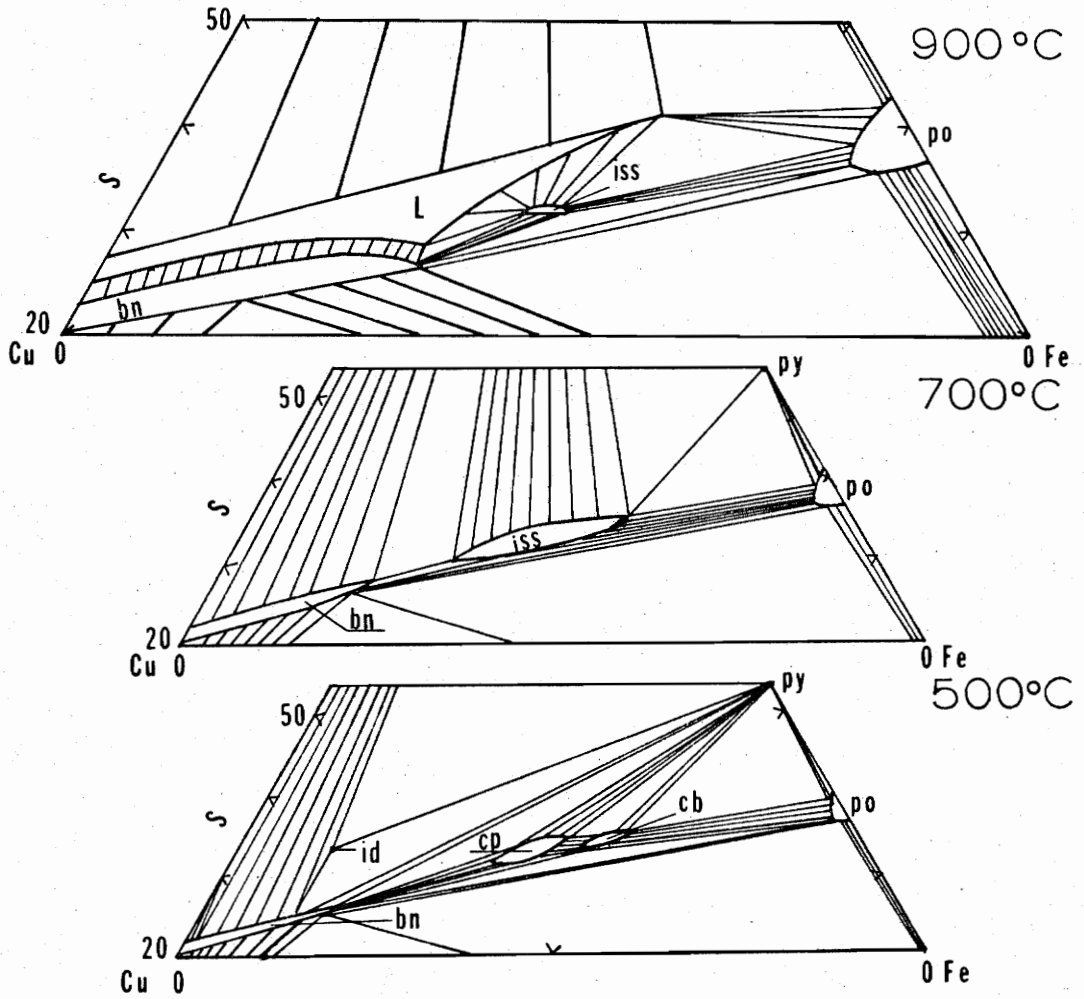

Figure 2. Condensed Phase Diagrams Illustrating the Relationships Between the Phases in Selected Portions of the Cu-Fe-S System at 500°C, 700°C, and 800°C. The 900°C isotherm is after Kullerud et al. (1969). The 700°C and 500°C isotherms are after Yund and Kullerud (1966).

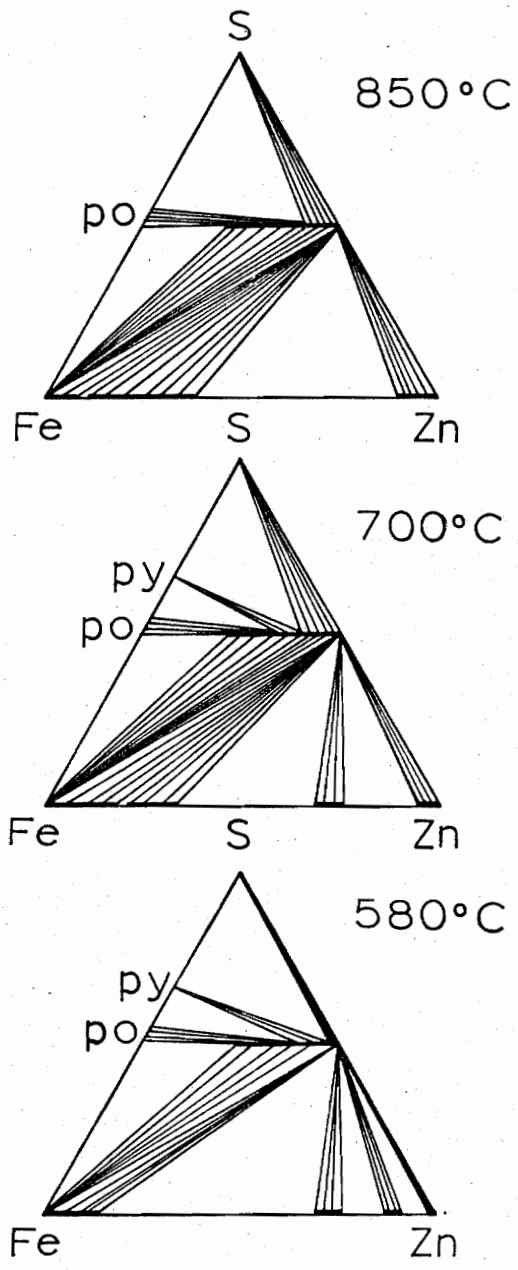

Figure 3. Condensed Phase Diagrams Illustrating the Relationships in the Fe-Zn-S System at 580°C, 700°C, and 850°C. After Barton and Toulmin (1966).

emphasis on the 500°C and 800°C isotherms (Figure 4). They reported a solid solution at 800°C of up to 7±1 mol percent ZnS in Cu_2S but of less than 1 mol percent Cu_2S in ZnS. At lower temperatures they found ZnS coexisting with all other phases as they became stable.

Cu-Fe-Zn-S. Previous investigations in the Cu-Fe-Zn-S quarternary system have concentrated on natural sphalerite and chalcopyrite assemblages. The intimate textural relations observed between these two phases led Schwartz (1931) and Nakano (1934) independently to attempt to define the temperature at which solid solution begins. Both researchers heated natural samples in open air up to 500°C and neither found evidence of solid solution. Buerger (1934) approached the problem by sealing the natural samples in evacuated Pyrex tubes and then heating them. He observed that chalcopyrite went into solid solution with sphalerite above the range 350°C to 400°C. The preceeding studies involved sphalerite as the major phase. In instances where chalcopyrite was the major phase, temperatures of solid solution have been reported by Borchert (1934) as being between 470°C and 550°C, by Nakano (1937) as being between 470°C and 480°C, and by Sugaki et al. (1955) at 500°C. In 1963 Barton and Toulmin demonstrated that in the Zn-Fe-S ternary system the presence of iron in the sphalerite structure increased the unit cell dimension in a linear fashion. Toulmin (1960), on the other hand, reported that the addition of copper to an iron-bearing sphalerite decreased the size of the sphalerite unit cell.

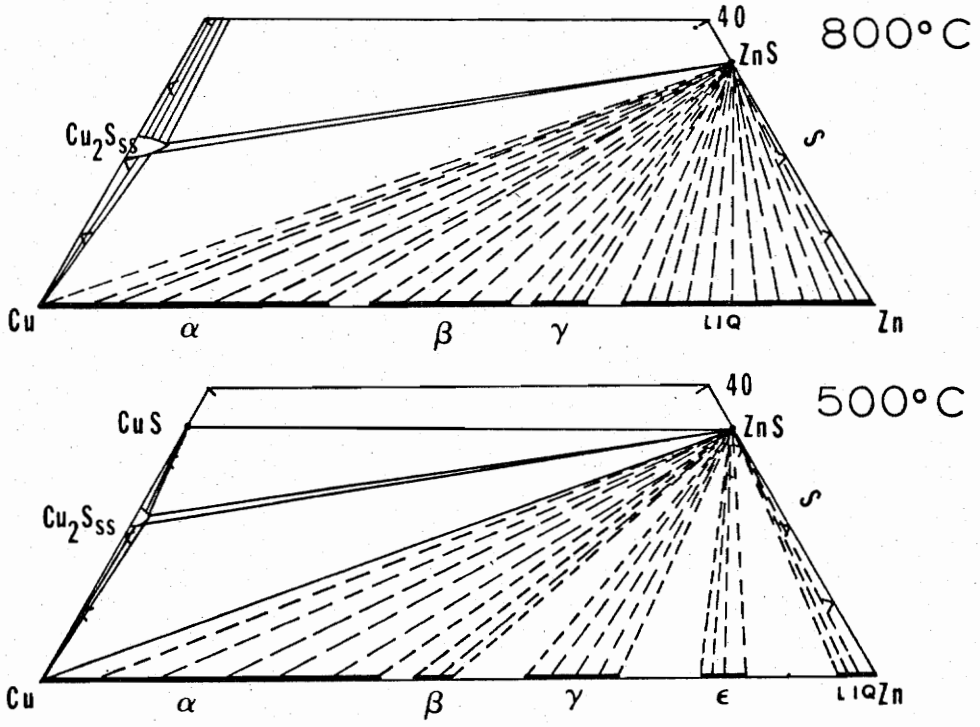

Figure 4. Condensed Phase Diagrams Illustrating the Phase Relationships in the Cu-Zn-S System at 800°C and 500°C. After Craig and Kullerud (1973).

EXPERIMENTAL TECHNIQUES AND MATERIAL

The investigation was conducted using ASARCO 99.999+ percent purity Zn, Cu, Fe, and S. Iron sponge was heated in a stream of hydrogen to reduce any impurity oxides that may be present; the copper and zinc were in bar form, and the oxidized coatings were removed by filing prior to use. The starting materials were weighed ±0.05 mg on a Metler balance, and sealed in high-purity fused quartz tubing using the procedure outlined by Kullerud (1971). The sealed tubes were then reacted at 500°C for up to five days in horizontal, cylindrical furnaces of the type described by Kullerud (1971). A modified Hadidiacas controller regulated the temperatures within ±2°C, while calibrated chromel-alumel thermocouples were monitered by a Speed-o-max strip chart recorder and a Numatrom digital potentiometer.

After the initial reaction of runs at 500°C for five days, the tubes were removed from the furnaces and quenched in water. The contents were homogenized by grinding under acetone (to prevent oxidation) and split into 50 mg units which were sealed in silica tubing for further runs. The present study employed three series of experiments.

The first series, twenty-eight capsules containing compositions in the ZnS-CuS-FeS plane, was reacted at 800°C for two days, quenched, divided into four bundles, and placed in furnaces at 800°C, 700°C, 600°C, and 500°C for thirty days. The second series (of the same size and composition but with 20 wt. percent FeS_2 added)

followed an identical procedure but with a run time of forty days. The third series, composed of one hundred experiments, omitted the second reaction step used in the first and second series and immediately after homogenization was placed in furnaces at 800°C, 700°C, 600°C, and 500°C for thirty days, forty-five days, sixty-three days, and seventy days respectively. The run products were quenched in water, removed from the capsules, and split longitudinally. In each run half of the run product was mounted in epoxy with the long dimension parallel to the surface in order to expose a maximum amount of the material to reflected light observation and microprobe analysis. The remainder of the material was examined by x-ray diffraction.

Initial phase identification and observation was conducted by reflected light microscopy and checked by microprobe analysis and x-ray diffraction. The x-ray diffraction studies were conducted on a Norelco powder diffractometer. The microprobe analyses were performed on an ARL EMX-SM and the data reduction accomplished using the program EMPADR VII (Rucklidge and Gasparrini, 1969). The third series of runs contained pyrrhotite indicators, separated from the runs by silica wool, which were x-rayed with a silicon internal standard ($\underline{a}$ = 5.4035Å) to accurately determine the location of the (102) peak in order that the sulfur fugacity of the runs could be determined. This procedure was developed by Toulmin and Barton (1964).

From the third series of runs, on which fugacity determinations were conducted, a number of sphalerites above the troilite-iron sulfidation curve but below the pyrrhotite-pyrite sulfidation curve

were selected for powder diffraction analysis and subsequent unit cell determinations. This portion of the study permitted an observation of the effect of CuS on the unit cell of FeS-bearing sphalerite. The calculation of the cell dimension was accomplished by the LSUCR program written by Evans, Appleman, and Handwerker (1963).

One of the primary considerations in any study of this nature is to determine whether or not equilibrium has been attained. The two different approaches to the final reaction runs described earlier were an attempt to detect kinetic problems and, if possible, to circumvent them. The two procedures produce similar results through the temperature range 800°C to 500°C; therefore, either equilibrium existed or fortuitously the same pseudo equilibrium was achieved by two different methods over two different time spans. In the 500°C series, where the run time was more than twice as long as at 800°C, the coincidence of the phase boundaries in the same assemblages prepared by the two methods illustrates that equilibrium was likely attained.

The probability that equilibrium was attained is supported by the intergranular relationships observed in the polished sections. Figure 5 shows that the chalcopyrite-chalcopyrite interfaces as outlined by the exsolved sphalerite grains are roughly 120° at the intersection of three grains of the same material. Stanton (1972) reports that the 120° angle is an indication of equilibrium. These relationships are prevalent throughout the temperature range of this study and thus support the belief that equilibrium was attained in most of the experiments.

Many of the high temperature run products were apparently unstable when held at room temperature after quenching. Several charges, after their initial mounting, examination, and microprobe analysis, were set aside for a period of three weeks. At the end of that time re-examination revealed that a blue "tarnish" had formed on all of the copper-iron sulfides and the copper-rich sphalerites. In a few of the polished sections the same blue material was observed to have grown into the epoxy mount. Once the sections were repolished the blue material was identifiable as covellite. During the probing of some of the sphalerites with higher copper and iron contents, the count rates for copper and iron increased with time and iss material was observed forming under the electron beam. Apparently the heating effect of the electron beam was sufficient to cause a considerable diffusion of the elements. To avoid this effect short counting intervals were utilized and the beam was moved after each reading.

EXPERIMENTAL DATA

The phases encountered within the compositional volume at 800°C include sphalerite, intermediate solid solution (iss), bornite, and pyrrhotite. Figures 5, 6, and 7 are projections of the reaction products of the compositions CuS-FeS-ZnS, CuS-FeS-ZnS + 20 wt. percent FeS_2, CuS.93-FeS.93-ZnS.93 and CuS.86-FeS.86-ZnS.86 on the CuS-FeS-ZnS plane. Because all phase equilibria are projected to the CuS-FeS-ZnS plane, all solid solutions are referred to in terms of their sulfide components (i.e. CuS) rather than as simple metal contents.

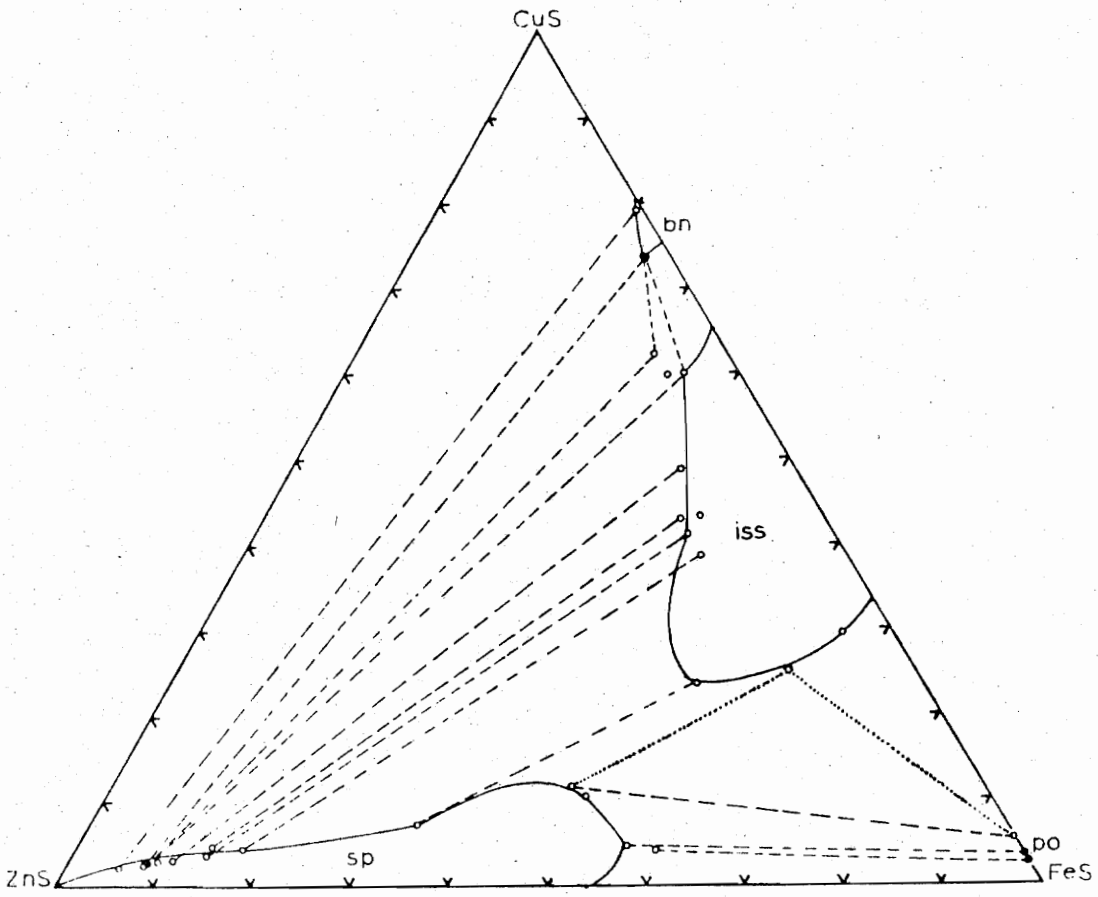

Figure 5. Projection of the Phase Equilibria in the S-region at 800°C on the CuS-FeS-ZnS Plane. The dotted line and circle represent a postulated assemblage not found in this experiment, but noted in others at lower temperatures.

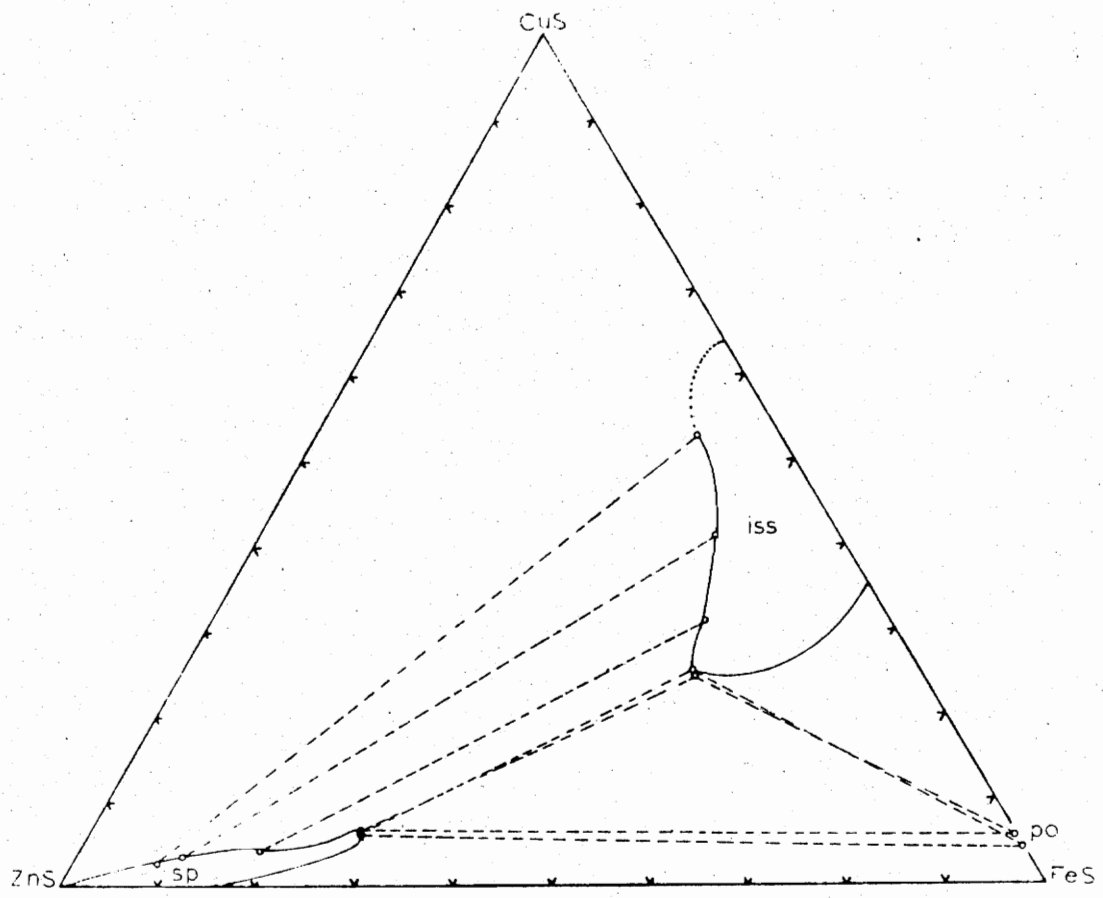

Figure 6. Projection of the Phase Equilibria in the Excess FeS_2 Region at 800°C on the CuS-FeS-ZnS Plane. The dotted line represents a theorized boundary of the phase field.

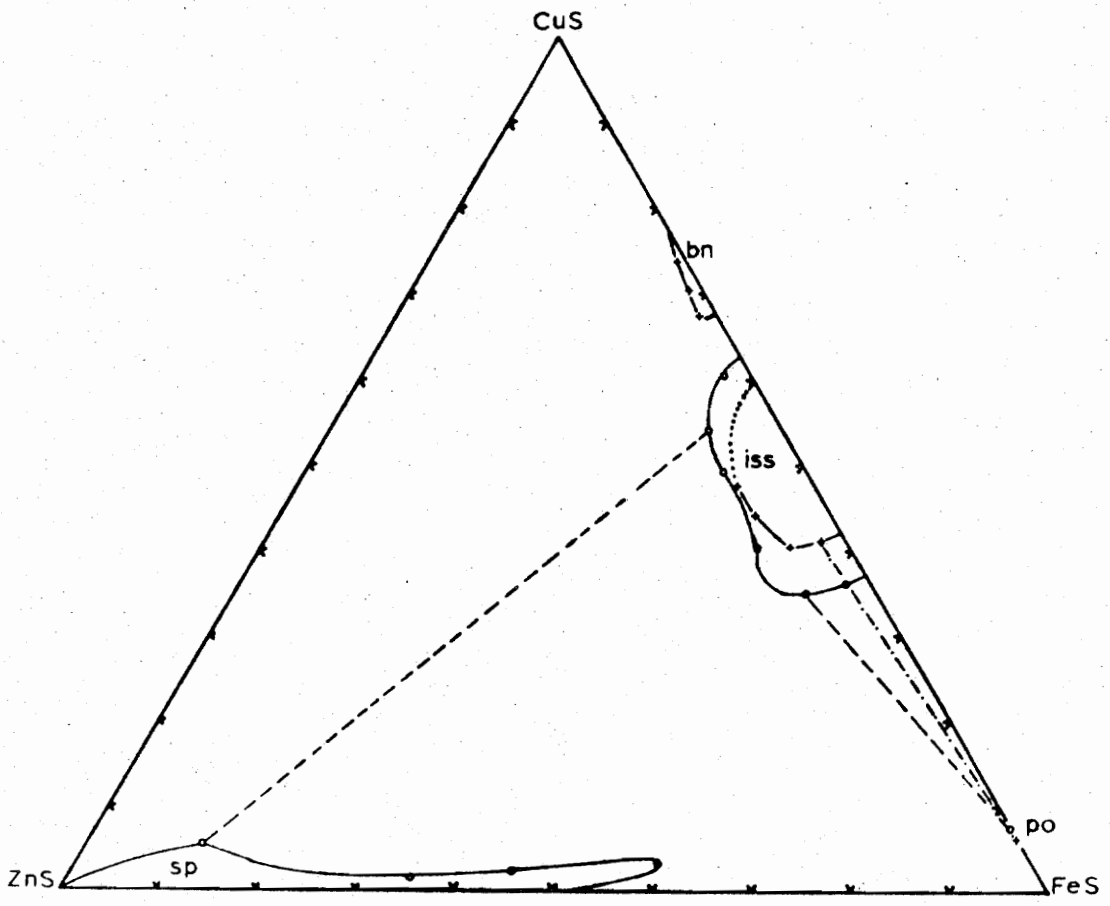

Figure 7. Projection of the Phase Equilibria in the S.93 and S.86 Regions on the CuS-FeS-ZnS Plane. The circles represent phases in the S.93 region. The pluses represent the phases in the S.86 region. Dotted lines are tie lines between phases in the S.93 region. Dashed-dotted lines are tie lines between phases in the S.86 region.

In Figure 5 the dotted line and circle indicate the postulated iss position even though it was not observed. Appendix I is a listing of the phase compositions obtained from microprobe analysis.

The bornite field accepts a maximum of 2.65 mole percent ZnS in solid solution in the S plane (although the microprobe analysis is given to two decimal places, only the first is considered significant). The only compositions which were sufficiently copper-rich to contain bornite were in the S and the S.86 planes. The portion of the bornite field observed in the S.86 plane demonstrates a shift to a lower CuS/FeS ratio than that observed in the CuS-FeS-ZnS plane. The bornites in the metal rich region display the various oranges, blues, and purples described by Yund and Kullerud (1966) as appearing in bornites in the pure Cu-Fe-S system. The compositional ranges observed at the various sulfur levels indicate that the solid solution of ZnS in bornite varies as a function of Cu/Fe and (Cu + Fe)/S ratios with the former having the stronger effect; i.e., there is .15 mol percent Zn observed in bornite of composition 44.69 mole percent Cu, 11.42 mol percent Fe and 43.74 mol percent S and 1.5 mol percent Zn in 41.78 mol percent Cu, 13,33 mol percent Fe, and 43.39 mol percent S. Hereafter, all compositional listings will be in mol percentages.

The longitudinal dimensions of the iss as inferred in this study and as interpolated from published diagrams of the pure Cu-Fe-S system are listed in Table 3A and 3B. In the presence of excess S the iss exhibits a maximum ZnS solubility of 22.69. The solubility of ZnS in the iss, as in the bornite volume, is a function of metal:metal

and metal:sulfur ratios. The maximum solubility limits of FeS and CuS in the sphalerite field are 55.75 and 11.47 in the S plane. In the presence of excess sulfur, however, the solubility of CuS in sphalerite is reduced to 6.09 and that of FeS in sphalerite to 27.9. The reduction of the sulfur content to S.93 results in a maximum CuS and FeS contents in the sphalerite of 5.98 and 55.75 respectively. The fourth solid solution field observed at 800°C was pyrrhotite. This field has a solubility of less than 0.5 for ZnS in all planes but may accept up to 7.19 CuS in the S plane and 1.64 CuS in the S.93 plane.

The phases in the S and the +20 wt. percent FeS_2 planes demonstrate that as the copper content of the copper sulfides increases both the copper and iron content of the coexisting sphalerite decreases. Free Cu and Fe were present coexisting with sphalerite and bornite or sphalerite and iss (analysis of these phases proved unsatisfactory as a result of their small size).

Optical investigations revealed that the sphalerite, bornite, and iss which were rapidly cooled from 800°C contained well developed, but very fine, exsolution textures as illustrated in Figures 8 and 9. These relationships raise a question regarding the validity of the analyses and consequently the outlines of the observed phase volumes. The presence of these textures indicates that the solid solutions existing at 800°C were not completely quenchable. An attempt to reconstruct the composition of the solid solution phase must include a volume averaging of the exsolved phases. Since the

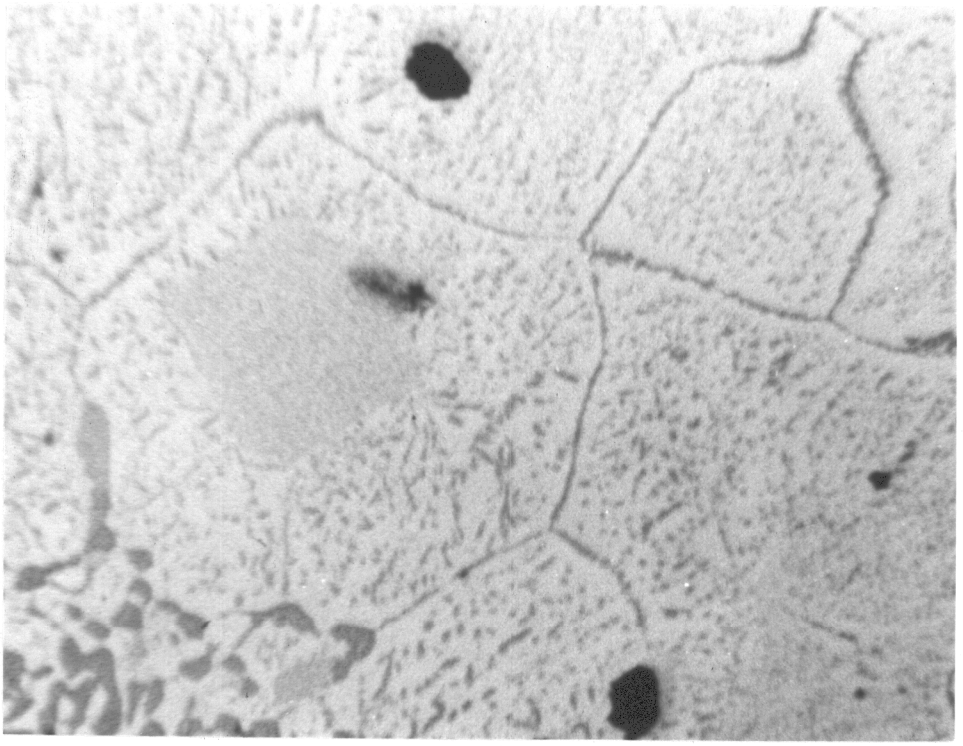

Figure 8. Run One at 800°C. Run one illustrates the concentration of sphalerite exsolution textures in iss. The intergranular boundaries as outlined by the sphalerite display 120° angles. The scale is .04 mm per inch.

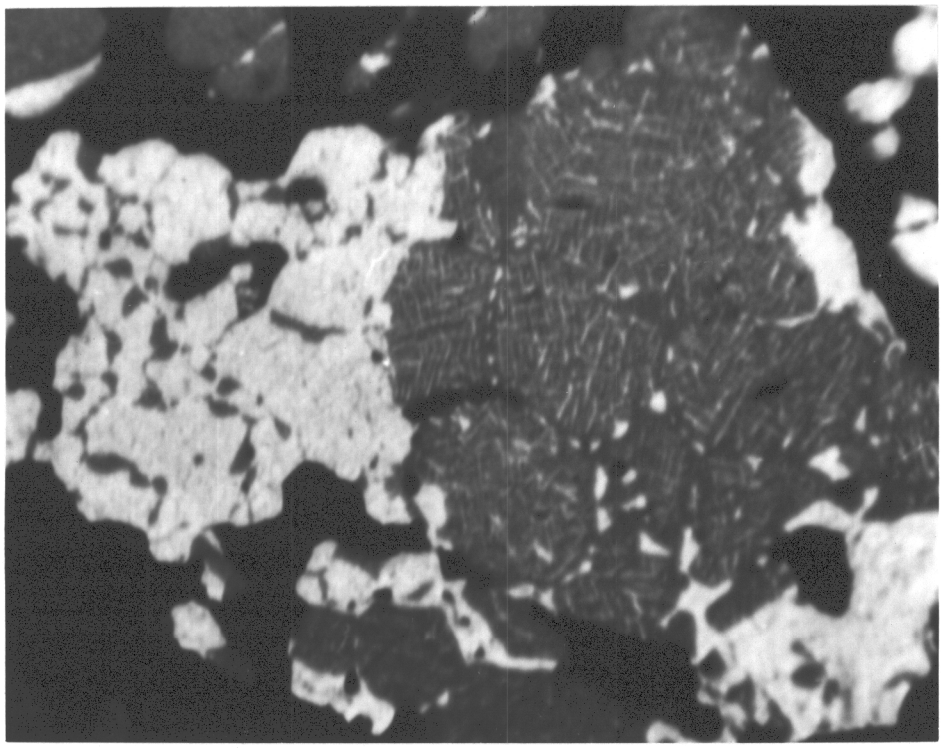

Figure 9. Run Six at 800°C. Run six illustrates the concentration of iss in sphalerite. The scale is .03 mm per inch.

volume of x-ray excitation by the electron beam of the microprobe is larger than the features under consideration, the analysis is actually an average of those phases within this volume. Figures 8 and 9 are illustrations of the density of the exsolution population in runs 1 and 6. The analyses of sphalerite, iss, and pyrrhotite in these two runs yield identical compositions within the standard error.

The 700°C isotherm (Figures 10, 11, 12) exhibits the same four solid solution volumes present as at 800°C (bornite, iss, pyrrhotite, and sphalerite); however, the relationships are somewhat more complicated because pyrite, now a stable phase, may coexist with each of the solid solution fields.

The bornite solid solution field at 700°C in the S plane accepts up to 1.5 ZnS. Bornite was not observed in the presence of excess FeS_2; these findings are compatible with the observation of Yund and Kullerud (1966) that pyrite and bornite are not stable together at this temperature in the pure Cu-Fe-S system. The decrease in effective sulfur to S.86 maintained the same trend as observed at 800°C in which the segment of the bornite field encountered in the S.86 plane was located at a lower CuS/FeS ratio (71.27/27.69) than it was in the S plane (76.27/23.20). These bornites also coexisted with free metal and displayed the pale colors noted at 800°C.

The iss volume demonstrates a maximum solid solubility of 16.0 for ZnS at a CuS/FeS ratio of 23.7/60.3. The logitudinal dimensions of the iss are compiled in Table 3A. A comparison of Tables 3A and 3B reveals that the addition of ZnS has extended the FeS-rich end

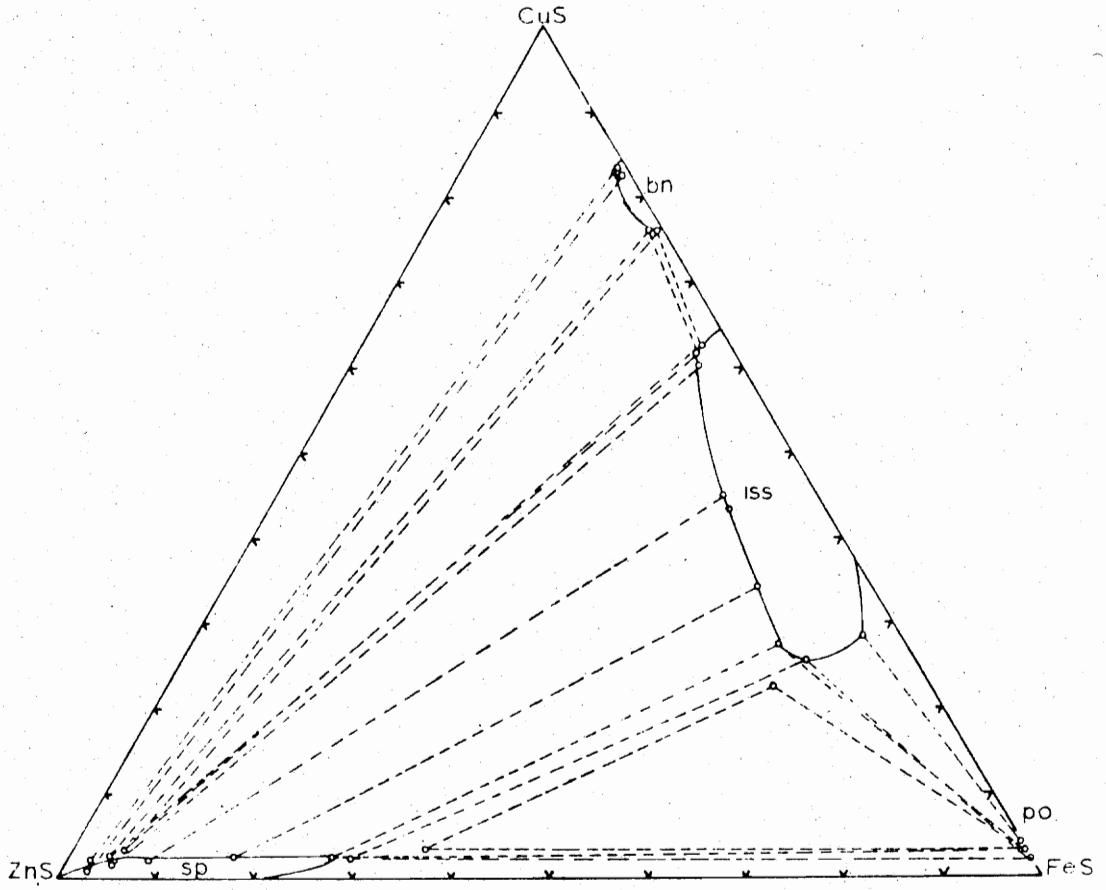

Figure 10. Projection of the Phase Equilibria in the S Region at 700°C in the CuS-FeS-ZnS Plane.

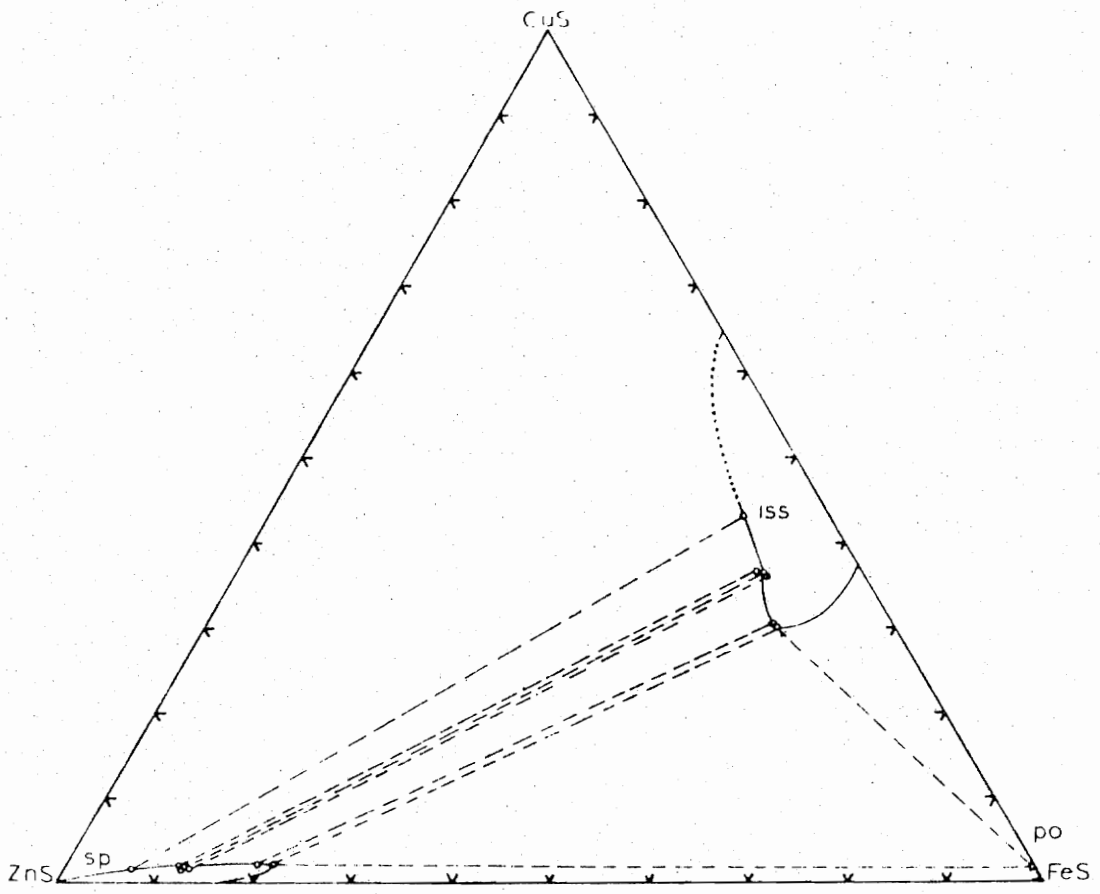

Figure 11. Projection of the Phase Equilibria in the Excess FeS_2 Region at 700°C on the CuS-FeS-ZnS Plane. The dotted line represents a theorized boundary of the phase field. Dotted circle represents a phase identified in polished section but not analyzed (postulated point).

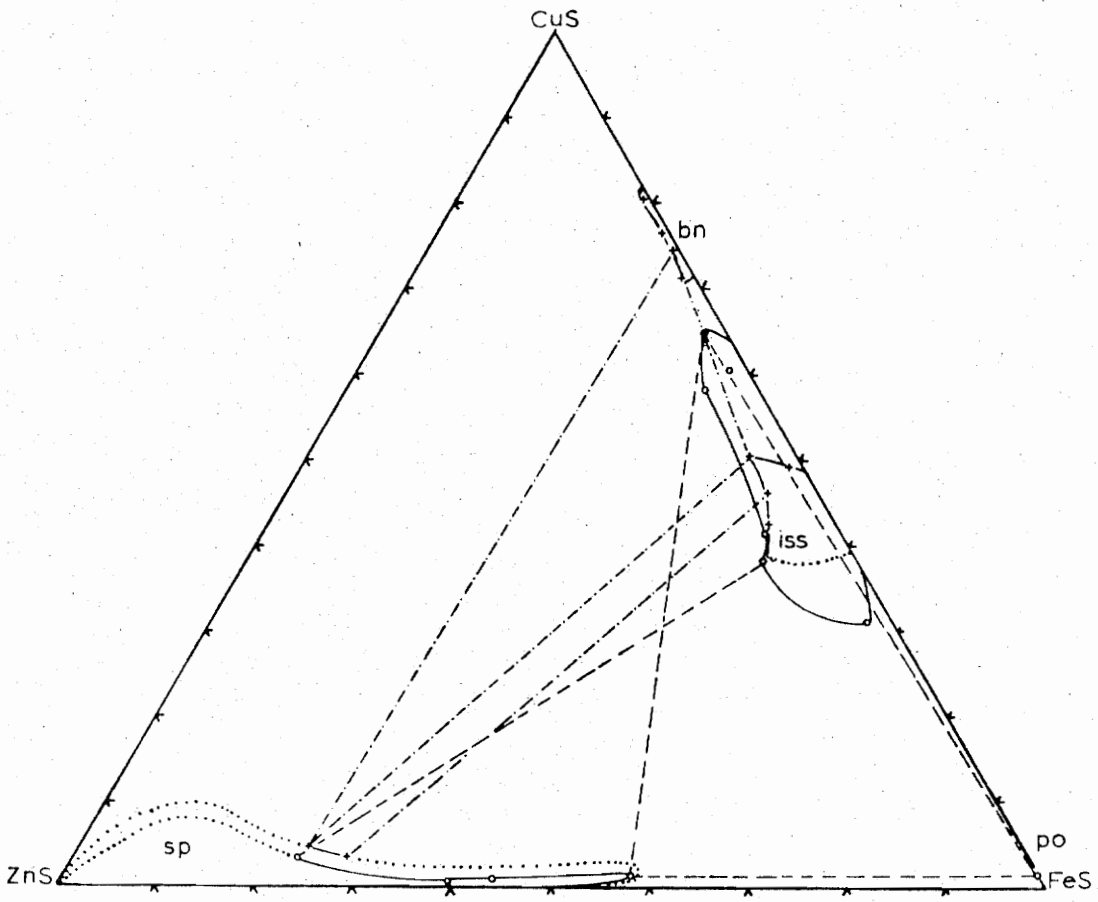

Figure 12. Projection of the Phase Equilibria in the S.93 and S.86 Regions at 700°C on the CuS-FeS-ZnS Plane. The circles represent phases in the S.93 region. The pluses represent phases in the S.86 region. Dashed lines are tie lines between phases in the S.93 region. Dotted lines represent a theorized boundary of the phase field.

of the iss but has had little effect on the composition of the CuS-rich end. The ZnS content of the iss volume is not appreciably altered in the excess FeS_2 region or in the sulfur deficient (S.93 and S.86) regions. The sphalerite solid solution volume demonstrates a maximum solid solubility of 3.5 for CuS and 26.5 for FeS in the CuS-FeS-ZnS plane. The maximum solubility of FeS in sphalerite in the sulfur deficient region is 57.23, a slightly higher value than that observed in the pure Fe-ZnS system (54.3). In the low sulfur region (S.93-S.86) an increase in the FeS content of the sphalerite is accompanied by a decrease in the CuS content.

The phases pyrite and pyrrhotite exhibit the smallest volumes in the ZnS-CuS-FeS system. Pyrite at 700°C does not contain detectable Cu or Zn whereas pyrrhotite contains a maximum of 4.0 CuS and 0.5 ZnS.

The coexisting phases in the sulfur deficient region exhibit assemblages which appear to be in disequilibrium as evinced by crossing tie lines. The method of projection chosen to illustrate the phase relations among the Cu-Fe-Zn sulfides unfortunately presents the appearance of disequilibrium in Figure 12. It must be borne in mind however that the relationships presented are actually three-dimensional and not two-dimensional as the projection suggests. The phases in the S plane demonstrate that in coexisting Cu-Fe-S and sphalerite an increase in the Cu content in the Cu-Fe-S is accompanied by a decrease in the Fe content of the sphalerite and an increase in the CuS content of the sphalerite.

The phases present in the Cu-Fe-Zn-S volume of interest at 600°C (Figures 13, 14, 15) are the same as those at 700°C: bornite, iss,

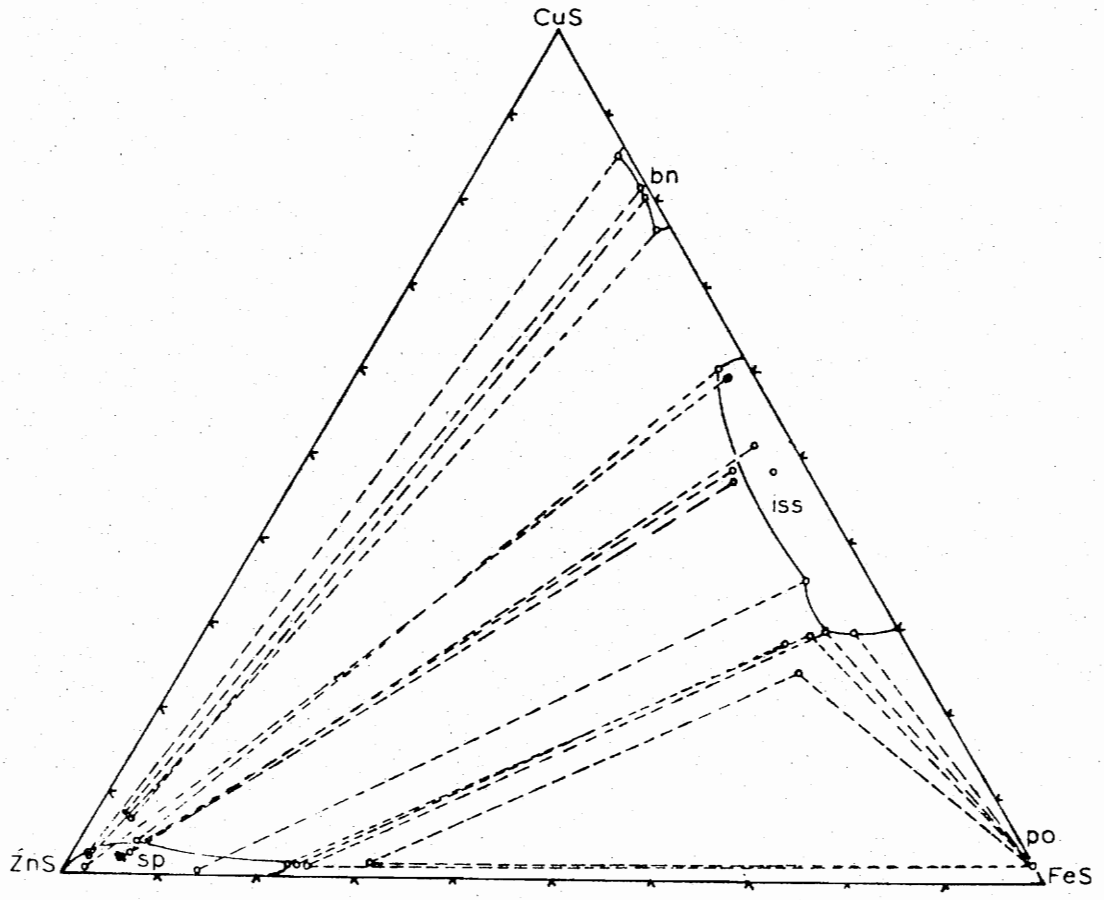

Figure 13. Projection of the Phase Equilibria in the S Region at 600°C on the CuS-FeS-ZnS Plane.

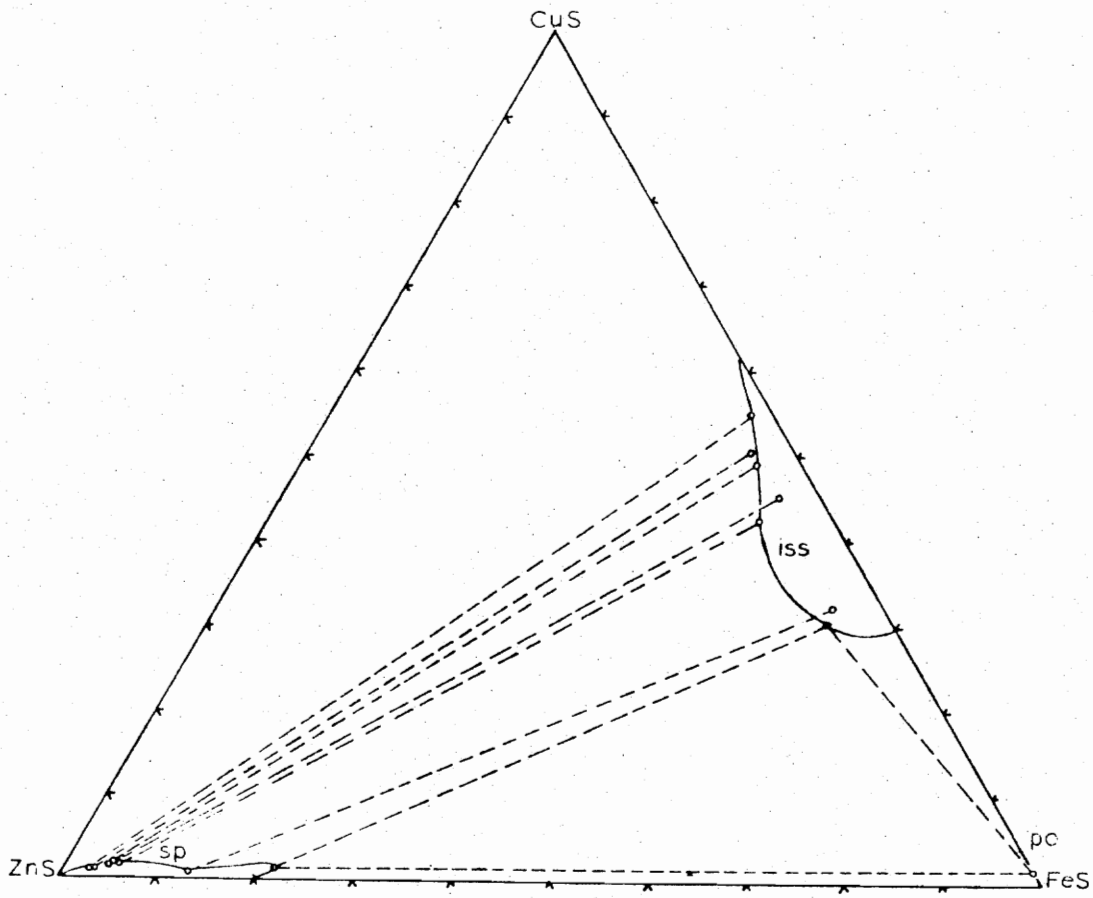

Figure 14. Projection of the Phase Equilibria in the Excess FeS_2 Region at 600°C on the CuS-FeS-ZnS Plane.

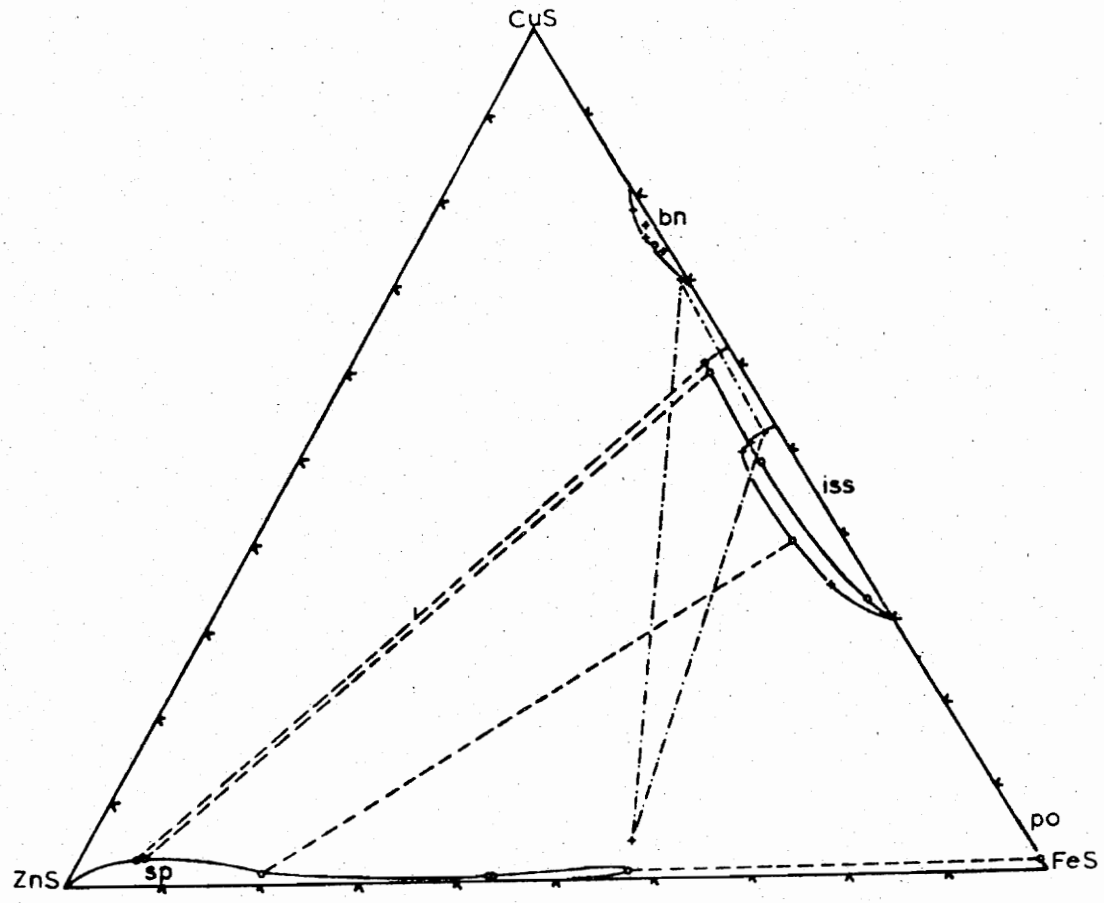

Figure 15. Projection of the Phase Equilibria in the S.93 and S.86 Regions at 600°C on the CuS-FeS-ZnS Plane. The circles represent phases in the S.93 region. The pluses represent phases in the S.86 region. Dashed lines are tie lines between phases in the S.93 region. Dashed-dotted lines are tie lines between phases in the S.86 region.

pyrrhotite, pyrite, and sphalerite. The bornite volume encountered has expanded along the CuS-FeS join in both directions. The maximum solubility of ZnS at 600°C is 2.0 and occurs at a CuS/FeS ratio of 76.28 to 21.97. As at 700°C, bornite is absent in the excess FeS_2 region, an observation compatible with the findings of Yund and Kullerud (1966). In planes of reduced sulfur content the bornite volume is located at lower CuS/FeS ratios; this shift is similar to those observed at 800°C and 700°C. The shift parallel to the CuS-FeS join and does not result in any change in the solubility of ZnS.

Solubility of ZnS in iss is 8.23 at 600°C, a decrease from the value observed at 700°C (Table 2). The observed longitudinal dimensions of the iss are presented in Table 3A. Comparison with the dimensions of the iss in the Cu-Fe-S system (Table 3B) demonstrates little difference between the two values indicating that the ZnS solubility of the iss no longer causes the extensive distortion of the Cu/Fe configuration of the Cu-Fe sulfides observed at 800°C and 700°C. In the presence of excess FeS_2 the ZnS content of the iss is reduced to a maximum of 7.44 (which occurs at a CuS/FeS ratio of 42.91 to 49.64).

In the S.93 the iss accepts a maximum of 4.95 ZnS (at a Cu/Fe ratio of 39.19/55.86). The remainder of the field averages about 3.5 ZnS in width. Figure 15 illustrates that the two sulfur deficient planes intersect two portions of the iss field at the lower levels of the iss volume (see Figure 2 for a comparison).

As observed at 800° and 700°C the sphalerite and Cu-Fe-S phases maintain the same general relationship in which the FeS content of the

Table 2

The Maximum Solubilities in the Major Cu-Fe-Zn-S Solid Solution Phases (800°C-500°C)

	800°C	700°C	600°C	500°C
a. Mole Percent CuS in Sphalerite				
In the presence of excess sulfur	6.09	1.98	1.78	6.03
S	11.47	3.21	3.98	3.36
in the plane of .93 sulfur	5.98	3.28	3.51	4.32
in the plane of .86 sulfur	---	4.35	4.46	3.12
b. Mole Percent ZnS in Intermediate Solid Solution				
In the presence of excess sulfur	22.69	11.51	7.44	7.25
S	22.73	12.86	11.83	4.76
in the plane of .93 sulfur	9.40	8.77	4.14	2.86
in the plane of .86 sulfur	7.10	6.18	4.95	308
c. Mole Percent ZnS in Bornite				
In the presence of excess sulfur	---	---	---	.53
S	2.65	1.71	1.74	.52
in the plane of .93 sulfur	---	---	---	.63
in the plane of .86 sulfur	1.68	1.04	1.54	.51
d. Mole Percent FeS in Sphalerite				
In the presence of excess sulfur	27.90	20.95	21.31	19.27
S	55.75	26.18	22.56	19.16
in the plane of .93 sulfur	58.58	57.23	56.40	50.05
in the plane of .86 sulfur	---	---	55.97	50.31
e. Mole Percent FeS in Sphalerite of the Pure Fe-Zn-S System (from Barton and Toulmin, 1966)				
In the presence of excess sulfur on the Fe-Zn-S plane	15.83 between 15.83 & 55.66	16.50 between 16.50 & 54.33	20.00 between 20.00 & 52.66	22.83 between 22.83 & 51.50
in the presence of Fe	55.66	54.33	52.66	51.50

Table 3

	High CuS end (mol percent)	High FeS end (mol percent)
A. Observed Variations in the Length of the iss field with temperature projected on the CuS-FeS-ZnS plane in the Cu-Fe-Zn-S system		
800°C (Figure 2)	ZnS 5.55, CuS 60.26, FeS 34.20	ZnS 4.54, CuS 29.44, FeS 65.02
700°C (Figure 3)	ZnS 2.94, CuS 62.37, FeS 34.70	ZnS 3.81, CuS 28.59, FeS 67.50
600°C (Figure 4)	ZnS 2.97, CuS 60.48, FeS 36.54	ZnS 4.84, CuS 29.74, FeS 65.41
500°C (Figure 5)	ZnS 1.60, CuS 62.47, FeS 35.93	ZnS 5.16, CuS 26.56, FeS 68.28
B. Variations in the Length of the iss field with temperature projected on the CuS-FeS line in the Cu-Fe-S system		
700°C (Kullerud et al., 1969)	CuS 64.16, FeS 35.80	CuS 37.50, FeS 62.50
600°C (Cabri, 1973)	CuS 62.00, FeS 38.00	CuS 30.00, FeS 70.00
500°C (Yund and Kullerud, 1966)	CuS 61.17, FeS 38.83	CuS 35.55, FeS 64.45

sphalerite decreases with an increase of the CuS content of the coexisting Cu-Fe-S phase. The increase in CuS concentration in sphalerite with the increase in the CuS content of the coexisting Cu-Fe-S phases reported in the low sulfur planes at higher temperatures now is evident in the S plane.

The sphalerite solid solution field in the S plane has a maximum solubility of 22.56 for FeS at 76.23 ZnS and 1.20 CuS. The maximum solubility for CuS (3.98) is observed at 89.58 ZnS and 6.44 FeS. In the presence of pyrite the solubility of FeS in sphalerite is reduced to 21.31 and that of CuS to 1.98. The S.93 plane contains a sphalerite field with a solid solubility of 56.4 FeS and 3.51 CuS.

The two remaining phases exhibit limited solubilities for CuS and ZnS; and the solubilities appear insensitive to changes in sulfur pressure. The pyrrhotite solid solubility for CuS is 2.4 and for ZnS is less than 0.5. Pyrite in the two analyses has up to 1.88 CuS and in two other analyses has up to 2.0 ZnS in solid solubility. Because the size of the pyrite grains analyzed was less than 2 microns, the analyses showing these large Cu and Zn contents of the pyrite are deemed to be the result of the microprobe electron beam exciting the surrounding material.

The phases encountered within the compositional volumes at 500°C include sphalerite, iss, bornite, pyrite, pyrrhotite, and idaite (Figures 16, 17, 18). Chalcopyrite which is stable in its tetragonal form in the pure Cu-Fe-S system (Barton, 1973) was not observed in any Zn-containing experiments.

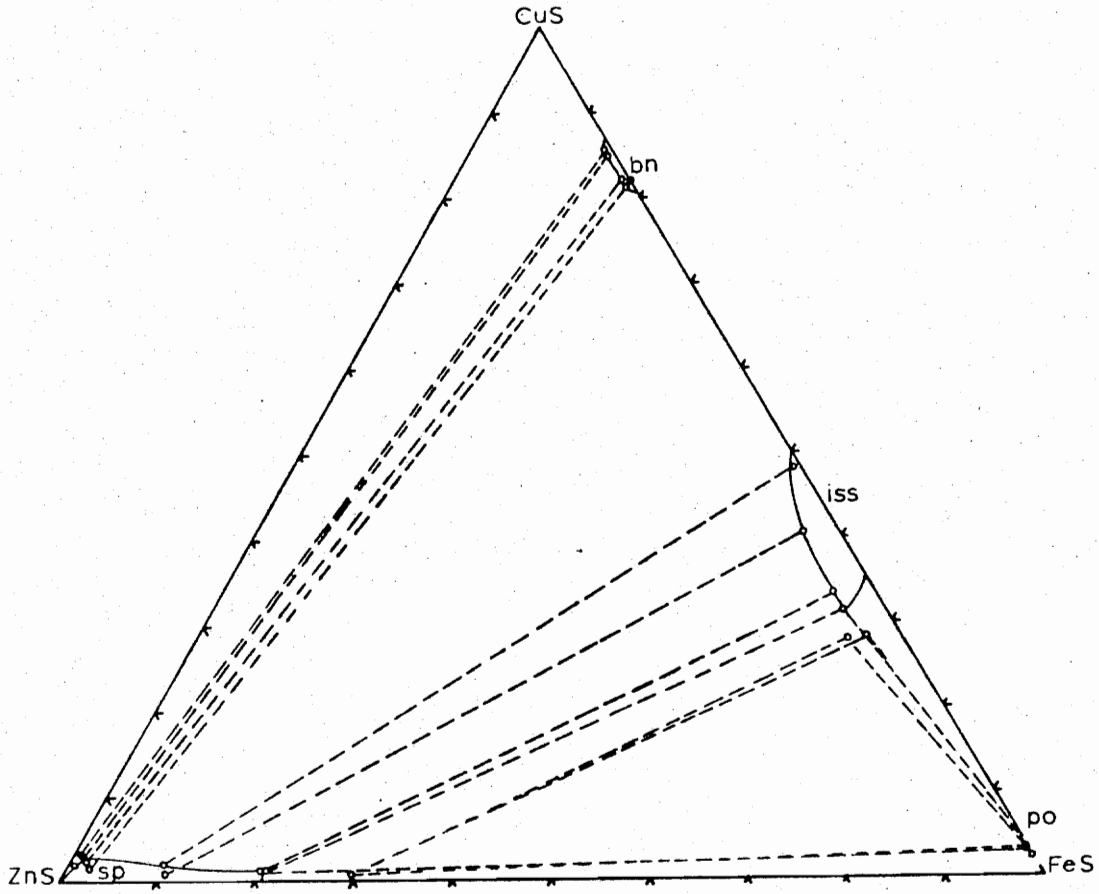

Figure 16. Projection of the Phase Equilibria in the S Region at 500°C on to the CuS-FeS-ZnS Plane.

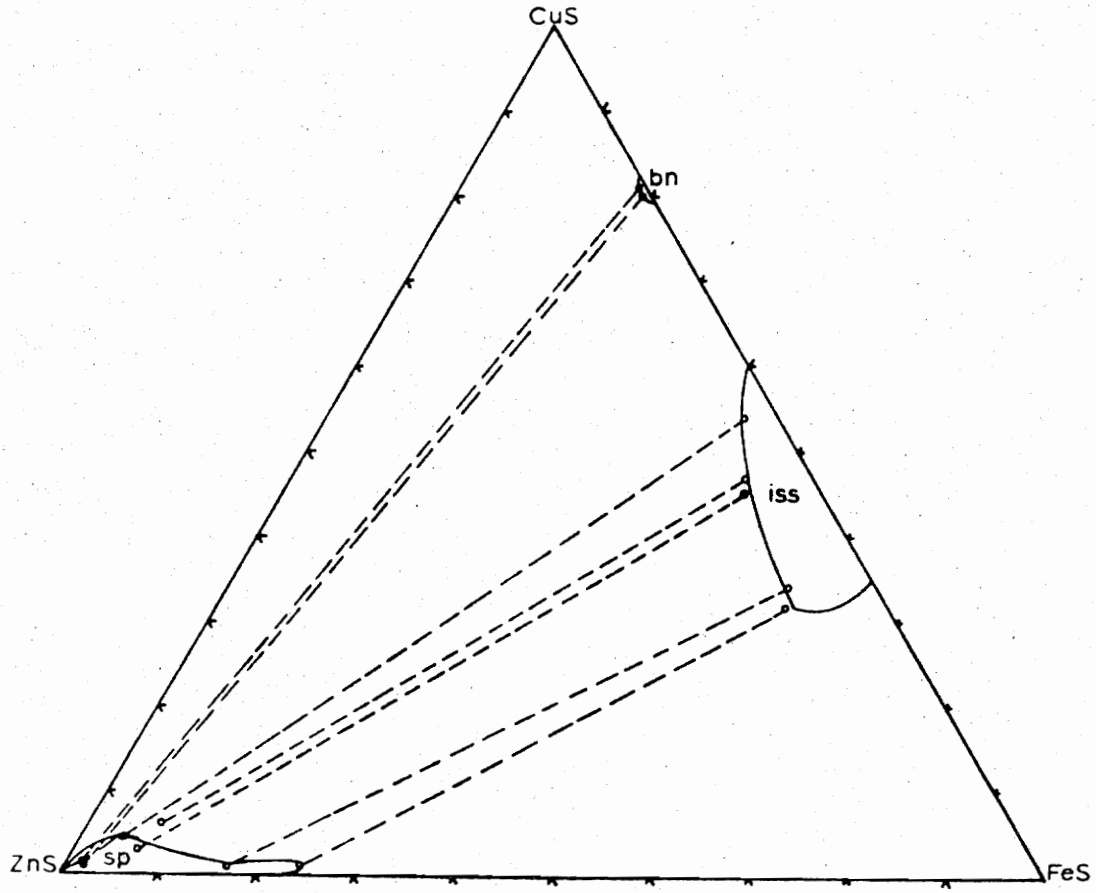

Figure 17. Projection of the Phase Equilibria in the Excess FeS_2 Region at 500°C on to the CuS-FeS-ZnS Plane.

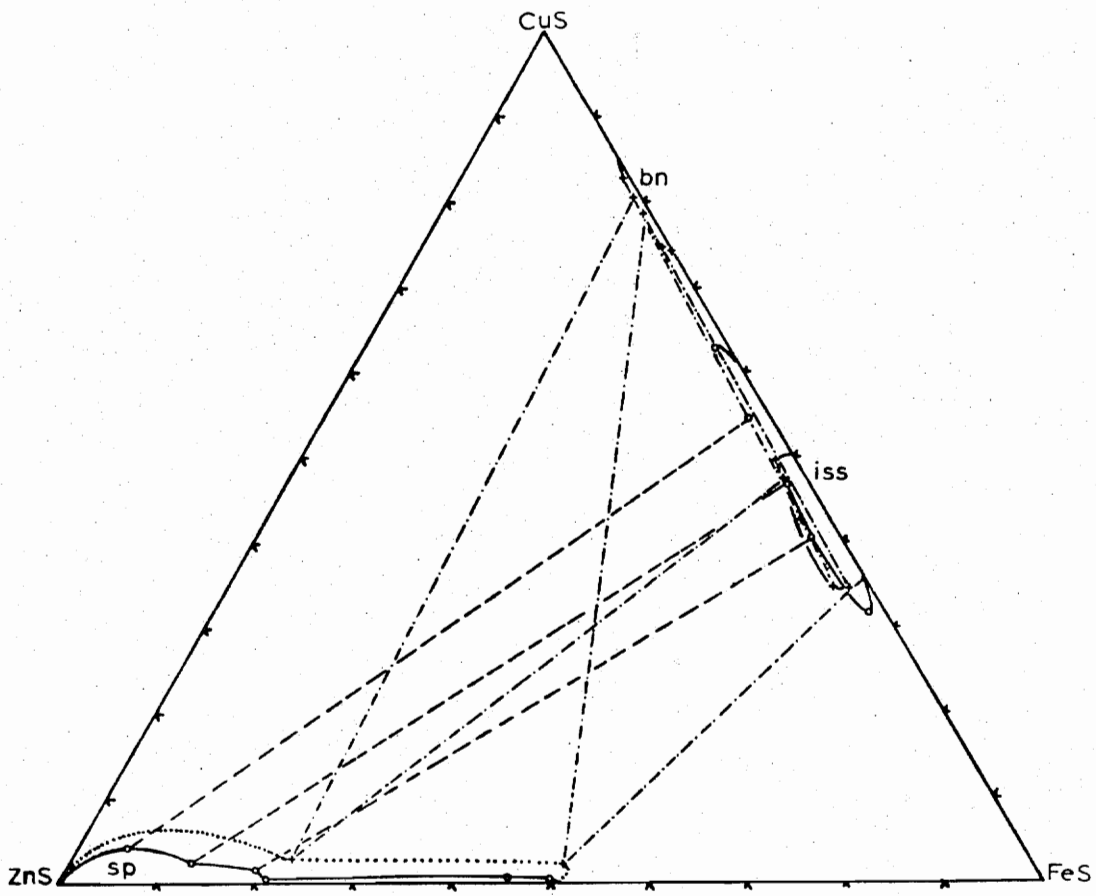

Figure 18. Projection of the Phase Equilibria in the S.93 and S.86 Region at 500°C on to the CuS-FeS-ZnS Plane. The circles represent phases in the S.93 region. The pluses represent phases in the S.86 region. Dashed lines are tie lines between phases in the S.93 region. Dashed-dotted lines are tie lines between phases in the S.86 region. Dotted lines represent a theorized boundary of the phase field.

The bornite solid solution volume displays a solid solubility of 0.53 ZnS at 85.63 CuS and 13.85 FeS. The addition of excess FeS_2 produced assemblages containing coexisting pyrite and bornite. Within the sulfur deficient planes (S.93 and S.86) the solid solubility of ZnS in bornite remains below 1.0.

The longitudinal dimensions of the iss in the pure Cu-Fe-S system indicates that although ZnS is taken into solid solution it does not drastically alter the shape or length of the iss field. The maximum solubilities of ZnS in iss are listed in Table 2 as 9.37 in the excess FeS_2 plane, 4.67 in the S plane, 2.86 in the S.93 plane, and 3.08 in the S.86 plane. These values break the established trend of the higher temperature isotherms in which variations of sulfur pressure from S decreased the solubility of ZnS in iss. Here the solubility is at its maximum in the +20 wt. percent FeS_2, decreases in S and is at a minimum in the low S region. The 500°C isotherm is the region in which kinetics may have a noticeable effect. Three experiments from series one are not considered in the CuS-FeS-ZnS diagram (Figure 16) because of major departures from trends established by the bulk of the experiments. In extracting series one from the furnace at 500°C three run capsules were noted as having slipped from their bundle and had probably been reacted at a lower temperature as a result.

The sphalerite solid solution field demonstrates a maximum solid solubility of 2.27 for CuS and 31.22 for FeS. Although one experiment indicated a maximum solubility of 6.03 CuS in the sphalerite, the value of 2.4 is considered far more likely in view of the trends established. The lone value of 6.03 is deemed either as nonequilibration

or a contaminated analysis. The decrease in available sulfur to the S.93 plane decreases the solubility of FeS in ZnS to 50.05 and the solubility of CuS in ZnS to 4.32. As at 600°C the negative correlation between CuS and FeS concentrations is observed here. In the S.86 plane the volume of the sphalerite field is enlarged toward CuS, but maintains the same FeS concentration as in the S.93 plane. While only two points are located along the sphalerite field in the S.86 plane the trend of negative correlation between FeS and ZnS may be observed as in the S.93 plane.

The phases pyrite and pyrrhotite appear to demonstrate limited solid solubilities for CuS and ZnS. No solubility for ZnS was detected in pyrite; but it would accept 2.8 CuS. In most analyses pyrite is pure FeS_2 and the incidence of CuS-bearing pyrites is attributable to the same contamination effect described earlier. Pyrrhotite is observed to accept 2.25 CuS but less than 0.5 ZnS in solid solution. The sulfur pressure variations have little effect on the solubilities of CuS and ZnS in pyrrhotite.

Idaite is present in the CuS-FeS-ZnS plane as a stable phase at 500°C. The structure of idaite in this plane is hexagonal, unlike any of the other phases at this temperature. The solubility of ZnS is less than 0.1 mole percent, probably because of the ordered hexagonal structure.

The sulfide deficient region S.86 again demonstrates that the diagrams which appear in the projections as planes are actually volumes which are composed of a "stack" of three phase assemblages. These

assemblages are hinged along the sphalerite solid solution volume (which does not vary measurably from a metal (Cu + Fe + Zn)/S ratio of 1/1).

DISCUSSION OF SYNTHETIC EXPERIMENTS

Two important circumstances apparently account for the solid solution between sphalerite and iss in the Cu-Fe-Zn-S system. First, the iss and sphalerite are similar as both are cubic and possess the sphalerite structure type with unit cell dimensions of $\underline{a} \simeq 5.43\text{Å}$ for iss (dependent on composition) and $\underline{a} = 5.4093\text{Å}$ (for pure ZnS). In sphalerite the cell dimension increases as FeS concentration increases (Appendix II). At temperatures below 557°C (Barton, 1973) the chalcopyrite becomes a stable phase; it is tetragonal and is composed of two of the iss unit cells so that $\underline{a} = 5.28\text{Å}$ and $c = 10.409\text{Å}$. No chalcopyrite was noted therefore the true effect of the transition in this system is not known. It is likely that chalcopyrite does not accept a significant amount of ZnS even at high temperature. This agrees with the observation of Buerger (1934) and Fujii's (1970) conclusions based on a review of the works conducted on natural Cu-Fe-Zn-S assemblages.

Secondly, the elements in their divalent state (IV coord.) have similar radii; Cu = 0.62Å, Fe = 0.63Å, and Zn = 0.60Å (Shannon and Prewitt, 1969). All of the above radii are within 15 percent variation limit outlined by Goldschmidt (1954) in his three rules

of solid solution. The similarity of these radii facilitate the various Cu-Fe-Zn substitutions observed in the range 800°C - 500°C and possibly over a much wider temperature.

The 800°C isotherm exhibits three notable features. In a region of high sulfur vapor pressure (Appendix III, runs 22, 30, and 31) the FeS content of the sphalerite is substantially above the 25 or 30 mole percent concentration suggested by Barton and Toulmin (1966) in the pure Fe-Zn-S system. The anomolous FeS concentration may be attributed to the positive correlation which exists between CuS and FeS in the sphalerite solid solution. The substitution of Fe for Zn causes expansion of the unit cell as illustrated by the increase in the sphalerite cell size. The substitution of Cu for Zn, however, decreases this effect in a FeS-bearing sphalerite by reducing the unit cell size (see Appendix II). Thus perhaps the coupled substitution of FeS and CuS allows more FeS to enter into the sphalerite solid solution. The second important feature is an extension of the iss field along the FeS 50 mole percent isopleth to an ZnS content of 29.73. The last feature to note in the 800°C isotherm is an extension to the sphalerite field along the 50 mole percent isopleth toward the iss to a CuS content of 11.74.

The structures of both iss and sphalerite are basically the same (as noted above). In iss the size difference between Fe and Cu is enough to allow extensive substitution of Zn for Cu. In the sphalerite field the coupled substitution has extended the field past the FeZnS point. Thus, it appears that the extension of the sphalerite field

along the 50 mole percent FeS isopleth is an expression of CuS substitution for ZnS, whereas the extension of the iss field along the same isopleth is an expression of the substitution of ZnS for CuS. The trends indicate that at some higher temperature there may be complete solid solution between the iss and sphalerite with the compositional variations expressed by $(Cu_{1-x}Zn_x)FeS$. However, Kullerud et al. (1969) indicated that the minimum melting point of the $CuFeS_2$ field is 960°C; consequently, the solvus may intersect the solidus before the solid solution is complete. The substitution of CuS in the sphalerite field and the substitution of ZnS in the iss field have the net effect of reducing the free energy of the respective structures.

The paper by Toulmin (1960) on the effect of Cu on Fe-bearing sphalerite indicates that the presence of Cu decreases the dimensions of the unit cell (this is consistent with the difference of Cu and Fe atomic radii). The unit cell dimensions of a number of sphalerites from runs containing a pyrrhotite indicator were determined using silicon metal as an internal standard. The sphalerites selected were all in sulfur vapor pressure range above the Fe-troilite isobar. The positive correlation between ZnS and FeS is well documented in several sources; and the equation for the calculation of the a cell edge from a given mole percent FeS ($a = 5.4093 + .0005637(\%FeS) - 0.00004107(\%FeS)^2$) has been taken from Barton and Toulmin (1966). The change in a with the addition of CuS is substantial. The cell edge calculated for a sphalerite containing 55.75 FeS is $a = 5.438$Å. A sphalerite with the

same FeS content but with 4.61 CuS has an observed $\underline{a}$ of 5.412Å. Other cell edges are presented in Appendix II.

Analysis of the pyrrhotite indicators demonstrates in a general way that the pyrrhotite apex of the CuS-FeS-ZnS diagram is a low sulfur fugacity region relative to the other portions of the system encountered in this study (Appendix III). In an interesting manner the pyrrhotite indicator highlights the correlation between sulfur fugacity and the FeS content of sphalerite. At 700°C (Figure 10) three experiments contain the assemblage sphalerite, pyrrhotite, and iss. Microprobe analysis located the compositions of these phases as being three phase fields nesting within each other formed by the runs 31, 22, and 30 progressing from the outermost (run 31) inward. The pyrrhotite indicator shows that the sulfur fugacity decreases from 31 to 30 and at the same time the FeS content of the sphalerite field increases. These relationships are also observable at 600°C and 500°C. An effort was made to utilize the pyrrhotite compositions obtained through microprobe analyses of the first and second series of experiments to calculate the fugacities in those regions. The fugacity values obtained from the pyrrhotite indicators were checked against the fugacity values obtained by using the microprobe analyses of the same runs. Unfortunately, the pyrrhotites within the run products proved unsatisfactory as the two values varied greatly and apparently unsystematically, a factor attributable to the CuS content of the pyrrhotite.

The relationship between CuS and FeS in sphalerite is dependent on sulfur pressure and temperature. In the S plane at 800°C there

is a strong positive correlation between CuS and FeS. At 700°C this correlation is evident but is less pronounced. At 600°C and 500°C CuS and FeS concentrations appear to be unrelated. The addition of excess FeS_2 decreases the solubility of FeS and CuS in sphalerite but the observed slopes of the positive correlation seem unchanged from those exhibited in the CuS-FeS-ZnS plane. Reduction in the sulfur content to S.93 and S.86 increases the solubility of FeS in sphalerite, and the correlation between CuS and FeS is negative through the entire 800°C to 500°C range. This may indicate that in the low sulfur regions there is competition between Cu and Fe for the Zn site.

The variation of CuS, FeS, and ZnS in the major solid solution regions are listed in Table 2 by temperature and sulfur content. The last two segments of the table allow a comparison of the FeS concentrations in sphalerite in the presence of Cu-bearing phases relative to that in sphalerites in the pure Fe-Zn-S system. The presence of Cu increases the amount of Fe the sphalerite structure will accept in solid solution in all instances except one. This exception occurs at the sphalerite, pyrrhotite, pyrite boundary at 500°C; there the FeS content is less than that observed in the Barton and Toulmin study (1966). This is an indication that equilibrium may not have been achieved in this instance. All other indications are that FeS concentrations are greater than those reported by Barton and Toulmin in the Fe-Zn-S system (1966).

The solid solubility of ZnS in iss decreases with temperatures from 800°C - 500°C; such a decrease is possibly a function of an

increase in the degree of ordering in the iss structure. Below 557°C chalcopyrite appears in the pure Cu-Fe-S system. As no chalcopyrite was observed in the present study it is apparent that the addition of ZnS restricts the extension of stable chalcopyrite tie lines to other phases within the system. This calls attention to the work of Buerger (1934) who found the first indication of solid solubility near 400°C. Perhaps this first indication of solid solubility of chalcopyrite in sphalerite is in fact the lowest temperature of appearance of the iss phase along the chalcopyrite-sphalerite pseudo-join in the Cu-Fe-Zn-S system. This was also the conclusion of Fujii (1970) upon reviewing the works on natural assemblages in the Cu-Fe-Zn-S system.

NATURAL ASSEMBLAGES

Discussion of natural Cu-Fe-Zn-S assemblages is included for two reasons. First, the research that has been done on this system was prompted by observations of exsolution features like those in Figures 19, 20, and 21 and was conducted on natural materials containing these features. Secondly, the natural assemblages have the advantage of long periods of time for equilibration of phases at lower temperatures; however the color banding in sphalerite indicates that complete equilibrium is not always reached at low temperature.

Ore suites containing Cu-Fe-Zn-S assemblages were donated by a number of mines in Canada and the United States. Of these ore suites the sixteen listed in Appendix IV contain evidence of intimate

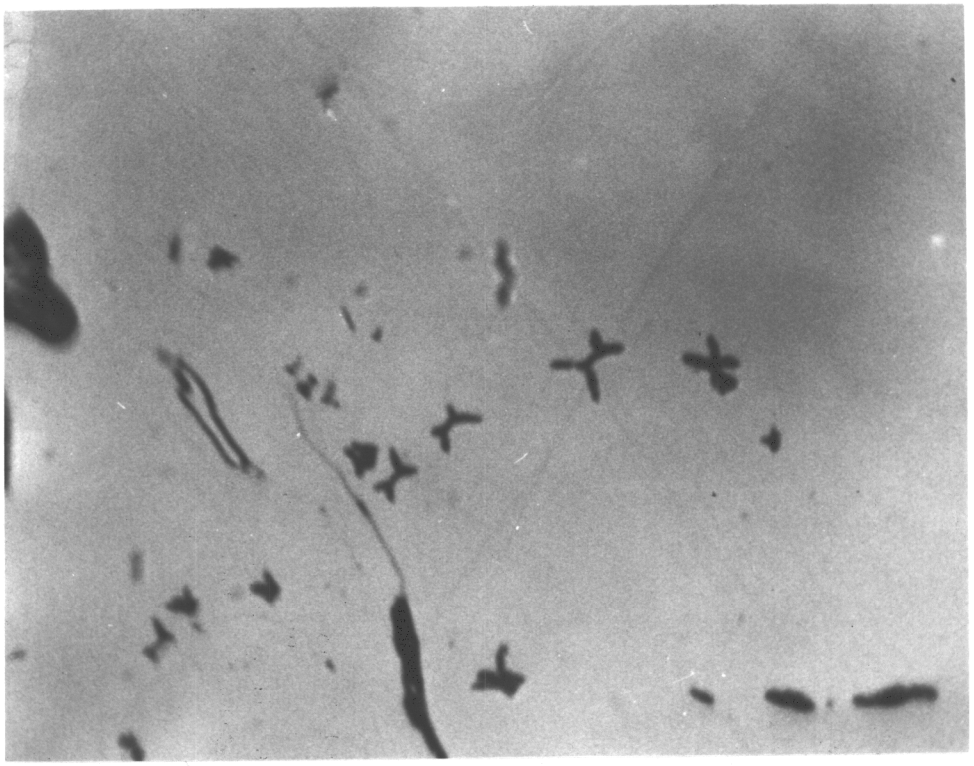

Figure 19. Sphalerite Stars in Chalcopyrite, Fox Lake Mine, Manitoba. The scale is .1mm per inch.

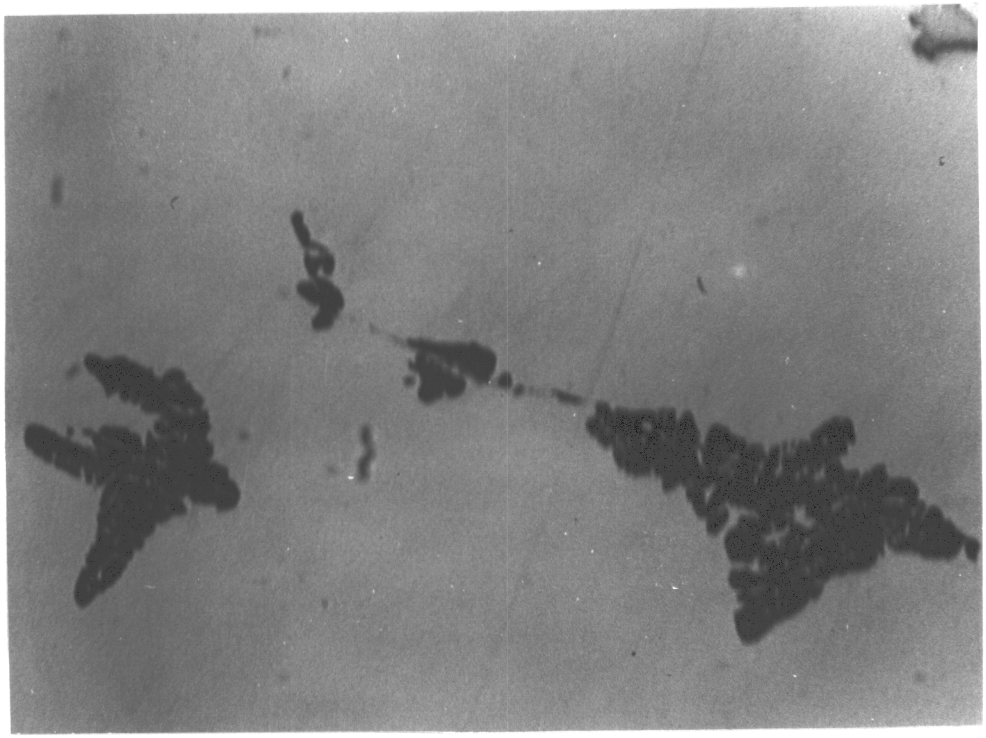

Figure 20. Sphalerite Stars in Chalcopyrite, Ruttan Mine, Manitoba. The scale is .7 mm per inch.

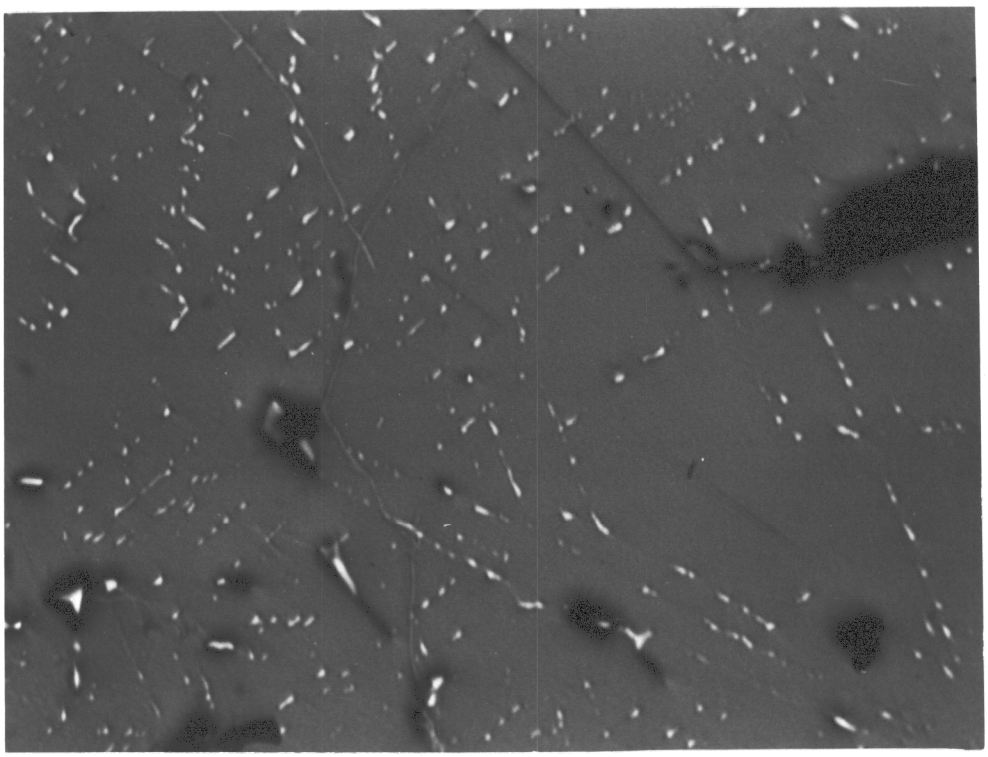

Figure 21. Oriented Chalcopyrite intergrowths in sphalerite, Sherritt-Gordon Mine, Manitoba. The scale is .4 mm per inch.

intergrowths between chalcopyrite and/or pyrrhotite and sphalerite representing replacement and/or exsolution. The zinc sulfides, iron sulfides, and the copper-iron sulfides were analyzed for Zn,Cu,Fe, and S. Appendix IV is a tabulation of the results; and Figure 22 is a plot of their relationships on the CuS-FeS-ZnS plane. The phases analyzed in the natural assemblages included cubanite, pyrrhotite, chalcopyrite, sphalerite, and pyrite. Bornite and idaite were not observed in any of the ore suites from the mines.

The sphalerites contained from 0.0 to 2.45 CuS and from 0.0 to 16.18 FeS. The pyrite did not contain detectable ZnS or CuS. Pyrrhotite analyses showed no copper; but several analyses did indicate the presence of ZnS in concentrations of up to 1.02. One cubanite (of the four analyzed) contained 0.41 ZnS. The sphalerites possessed between 0.4 and 17.79 FeS and between 0.0 and 0.44 CuS. The Cu and Fe variations in sphalerite appear to be independent of the coexisting mineral assemblage at the concentrations encountered in this study and may reflect other controls such as pressure.

These analyses demonstrate that as the phases cool to the ambient temperatures of their environment they tend to expel the materials once in solid solution. This is particularly evident when a crystallographic ordering is involved. The portion of the iss in the experimental work demonstrating the highest solubilities for ZnS is at the Cu/Fe ratio approaching that of cubanite. Interestingly, it is this portion of the iss which retains the cubic structure to the lowest temperatures in the pure Cu-Fe-S system (see Table 1). The change to the ordered orthrombic cubanite structure appears to decrease the solubility for ZnS from 22.7% at 800°C and 4.76 at 500°C to nearly 0.0 at room temperature.

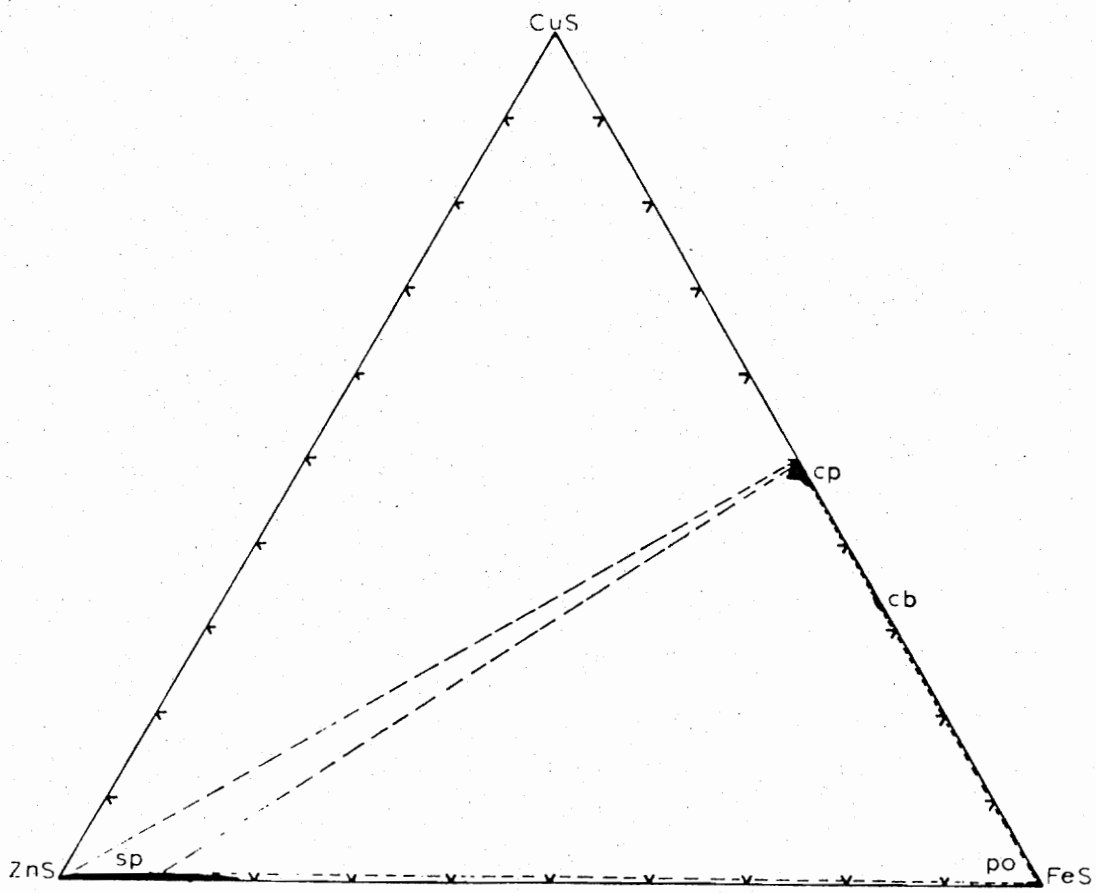

Figure 22. Projections of the Compositions of Natural Assemblages on the CuS-FeS-ZnS Plane.

SUMMARY AND CONCLUSION

1. The phases encountered during this study include bornite, intermediate solid solution, sphalerite, pyrrhotite, pyrite, idaite (only at 500°C), and covellite (which appeared as a post-quench product and was observed to have grown some distance into the epoxy).

2. Table 2 is a compilation of the maximum solubilities observed in the major solid solution fields (iss, sphalerite, and bornite) arranged by available sulfur and temperature. Trends of decreasing ZnS solubility in bornite with temperature and available sulfur are somewhat irregular when considered across the isotherms and planes. The primary control over the ZnS solubility in bornite is the metal:metal ratio within a given plane. As the CuS:FeS ratio approaches 5:1 the solubility for ZnS approaches a minimum.

In the iss the solid solution volume is sensitive to temperature and to a lesser extent to the availability of sulfur. The solubility of ZnS is more a function of the CuS:FeS ratio than it is a function of the metal:sulfur ratio; the ZnS solubility increases as the Cu/Fe ratio decreases from 2/1 to 1/2. The lack of any discernable trend in CuS solubility in sphalerite is an indication that there are several controlling factors other than temperature and sulfur pressure. The solubility of FeS in pure ZnS appears to be a function of both temperature and sulfur pressure. However, the maximum FeS solubilities in sphalerite are increased by the addition of CuS to the system over the temperature range 800°C to 600°C (Table 2).

3. Table 3A is a summary of the observed longitudinal dimensions of the iss field projected on the CuS-FeS-ZnS plane. Table 3B is a

collection of maximum longitudinal dimensions projected on the CuS-FeS line from Kullerud et al. (1969), Cabri (1973), and Yund and Kullerud (1966). There is a similarity between the lengths of the iss field in the Cu-Fe-S and Cu-Fe-Zn-S systems at 500°C and 600°C indicating that ZnS solubility does not distort the configuration of the Cu-Fe-sulfides. There is no previous work with which to compare the results in the 800°C isotherm.

4. The metastable nature of the bornite, iss, and sphalerite quenched at elevated temperatures is evident in the continued growth of corellite from these phases after quench. It is apparent that the extensive solid solutions at high temperature could never be preserved; in fact, very rapid re-equilibration from some compositions indicates that even the fine intergrowth textures observed experimentally would probably never even be evident in ores.

5. Natural assemblages containing chalcopyrite and sphalerite as well as various combinations of pyrrhotite, pyrite, and cubanite were analyzed. In the natural assemblages chalcopyrite demonstrated a maximum solid solubility for ZnS of 2.45 and sphalerite exhibited a solid solubility for CuS of 0.60.

6. The extensive solid solutions observed in this study result directly from the similarity of the sizes of the divalent Cu, Fe and Zn ions. In pure ZnS little or no solid solution with CuS was observed; however, as FeS is added, structural deformation results which allows the smaller Cu to enter the structure in a coupled substitution. The coupling in turn permits increase in the substitution of FeS and ZnS at high temperature.

The present reconnaissance study has elucidated the phase equilibria within the most geologically significant portion of the Cu-Fe-Zn-S system. Large mutual solubilities of ZnS in the Cu-Fe-S phases and Cu in Fe-bearing sphalerite have been demonstrated. The extent of the solid solubilities and their dependence on temperature and sulfur content (activity) clearly indicate that two mechanisms could be active in the formation of the intimate intergrowths noted between sphalerite and chalcopyrite:

1. exsolution due to decreasing temperatures
2. exsolution resulting from a drop or rise in sulfur activity

An additional mechanism clearly evident is the breakdown of the disordered iss from ordered chalcopyrite.

The large mutual solid solubility of ZnS and high temperature chalcopyrite-like phase (iss requires a re-examination of the concepts of CuFe and Zn separation at the magmatic stage. Previous concepts based on assumed small limits of solid solution appear erroneous. However, the differentiation of Zn relative to Cu and Fe could be a result of differences in volatility.

REFERENCES

Allen, C. T., and Crenshaw, J. L. (1912) The sulfides of zinc, cadmium and mercury: their crystalline forms and genetic conditions. Am. Jour. Sci., ser. 4, 34, 341-396.

Baker, Arthur, III (1960) Chalcopyrite blebs in sphalerite at Johnson Camp, Arizona. Economic Geology, 55, 387-398.

Barton, Paul B., Jr. (1973) Solid solutions in the system Cu-Fe-S. Part I: The CuS and CuFe-S joins. Econ. Geol., 68, 455-464.

——— and Toulmin, P., III (1964) Experimental determination of the reaction chalcopyrite + sulfur = pyrite + bornite from 350° to 500°C. Econ. Geol., 59, 747-752.

——————— (1966) Phase relations involving sphalerite in the Fe-Zn-S system. Econ. Geol., 61, 815-849.

——————— (1963) Sphalerite phase equilibria in the system Fe-Zn-S between 580°C and 850°C (abstract). Econ. Geol. 58, 1191-1192.

Borchert, H. (1934) Über Eutmischungenim System Cu-Fe-S und ihre Bedutng als Geologische Thermometer. Chemie der Erde, 9, 145-172.

Brett, Robin (1964) Experimental data from the system Cu-Fe-S and their bearing on exsolution textures in ores. Econ. Geol., 59, 1241-1269.

Bristol, Calvert C. (1974) Sphalerite geobarometry and some metamorphosed orebodies in the Flin Flan and Snow Lake Districts, Manitoba. Canadian Min., 12, 308-315.

Buerger, N. W. (1934) The Unmixing of Chalcopyrite from sphalerite. Amer. Min., 19, 525-530.

——— and Buerger, M. I. (1934) Crystallographic relations between cubanite segregation plates, chalcopyrite matrix and secondary chalcopyrite twins. Amer. Min., 19, 289-303.

Cabri, Louis J. (1967) A new copper iron sulfide. Econ. Geol., 62, 910-925.

——— (1973) New data on phase relations in the Cu-Fe-S system. Econ. Geol., 68, 443-454.

——— and Hall, S. R. (1972) Mooihoexite and haycockite, two new copper-iron sulfides, and their relationship to chalcopyrite and talnakite. Amer. Min., 57, 689-708.

Cabri, L. J., Hall, S. R., Sygmanski, J. T., and Stewart, J. M.(1973) On the transformation of cubanite. Canadian Min., 12,pt. 1.

Carpenter, R. H. and Desborough, G. A. (1964) Range in solid solution and structure of naturally occurring troilite and pyrrhotite. Amer. Min., 49, 1350-1365.

Cheney, Eric S. and Lange, Ian M. (1967) Evidence for sulfurization and the origin of some Sudbury-type ores. Mineralium Deposita, 2, 80-94.

Craig, James R. and Kullerud, Gunnar (1973) The Cu-Zn-S system. Mineralium Deposita, 8, 81-91.

Desborough, G. A. (1966) The Significance of accessory magmatic sphalerite in basic rocks to the origin of nickel ferous pyrrhotite ores. Econ. Geol., 61, 370-375.

Edwards, Austin Burton (1947) Textures of the ore minerals. Melbourne, Australasian Institute of Mining and Metallurgy, Inc.

Ehlers, Ernest G. (1972) The interpretation of geological phase diagrams: San Francisco, W. H. Freeman and Co.

Evans. H. T., Jr., Appleman, D. E., and Handwerker, D.S, 1963,The least squares refinement of crystal unit cells with powder diffraction data by an automatic computer indexing method (abstract). Amer. Crystallogr. Assoc., Cambridge, Mass., Ann. Meet., Program,42-43.

Friedrich, K. (1908) Die Zinkblende als Steinbiltner. Metallurgie, 5, 114-128.

Fujii, Takashi (1970) Unmixing in the system sphalerite and chalcopyrite, in Tatsumi, T., Volcanism and ore genesis. Tokyo University, Tokyo, 357-365.

Goldschmidt, V. M. (1954) Geochemistry (Alex Muis, Ed.), Oxford University Press, London.

Gruner, J. W. (1929) Structural reasons for oriented intergrowths in some minerals. Amer. Min., 14, 230-231.

Hadidiacos, Christos G., Howe, David A., Craig, James R., and Harris, Rae L., Jr. (1969) A low cost temperature unit for experimental petrologic studies. Journal of Geological Education, 17,35-37.

Hertel, Ludwig (1966) Rontgenographische und Mikrochemische Kontrolluntersuchwegen Bei Geochemischen Analysen an Eeinzetmineralin. Geologische Rundschau, 55, Sect. 2, 355-358.

Jensen, E. (1947) Melting relations of chalcocite: Avh. Norske Videnskakad. Oslo I. Math-Naturv. Kl., 6, 14.

Kissin, S. A. (1974) Phase relations in a portion of the Fe-S system. University of Toronto, 100.

Kullerud, Gunnar (1958) The Cu-S system. Carnegie Inst. Wash. Yearb., 57,215-218.

——— (1971) Experimental techniques in dry sulfide research in Ulmer, Gene C., Research techniques for high pressure and high temperature. Springer-Verlag, New York, 289-315.

——— (1953) The FeS-ZnS system, a geological thermometer. Norsk. Geol. Tidsskr., 32, 61-147.

——— and Yoder, H. S., Jr. (1959) Pyrite stability relations in the Fe-S system. Econ. Geol., 54, 533-572.

——— and Yund, R. A. (1960) Cu-S system (abstract). Geol. Soc. Amer. Bull., 71, 1911-1912.

——————— and Moh, G. H. (1969) Phase relations in the Cu-Fe-S, Cu-Ni-S, and Fe-Ni-S systems, in Wilson, H. D. B., Magmatic ore deposits, a symposium. Econ. Geol. Mon., 4, 323-343.

Lawrence, L. H. (1962) The mineral composition of the sulfide ores of the Drake and Rivertree Mining fields, New South Wales. The Australasian Institute of Mining and Metallurgy Proceedings, no. 201, 15-42.

Manning. P. G. (1966) Cu(11) in octahedral sites in sphalerite. Canadian Min., 8, 567-571.

Markham, N. (1961) Mineral composition of sulfide ores from the Peelwond, Cordillera and Mt. Costigan Mines, Peelwood District, N. S. W. The Australasian Institute of Mining and Metallurgy Proceedings, 199, 133-156.

Merwin, H. E., and Lombard, R. H. (1973) The system Cu-Fe-S. Econ. Geol. 32, 203-284.

Moh, G. H. (1960) Experimentelle Untersuchungen an Zinnkiesen und annalogen Germaniumverbindungen. N. Jb. Miner., Abh. 94,1125-1146.

——— and Kullerud, G. (1964) Phase relations at low temperatures: the Fe-S system. Carnegie Inst. Yearbk., 63, 207-208.

Morimoto, N. (1964) Structures of two polymorphic forms of Cu_5FeS_4. Acta Crystallogr., 17, 351-360.

Nakano, O., (1934) Change in microscopic intergrowth of chalcopyrite and zincblende by heatings. Jour. Jap. Assoc. Min. Petr. Econ. Geol., 12, 173-183.

———— (1937) Some experimental data on the micrographic intergrowth of chalcopyrite and zincblende. Jour. Jap. Assoc. Min. Petr. Econ. Geol., 18, 23-29.

Nesterov, V. N., and Ponomarev, V. D. (1960) The vapor pressure and activity of zinc sulfide in the ZnS-Cu_2S system at 1200-1400°C. Invest. Akad. Nauk. Kazakh. S. S. R., Ser. Met. Obogaschi Ogneup. No. 3, 64-72 (Chem. Abs. 55, 6115).

———————— (1958) Vapor pressure of zinc sulfide over the melts of ZnS-Cu_2S at 1000-1200°C. Akad. Nauk. Kazakh. S. S. R., Ser. Met. Obogaschi Ogneup., No. 3, 33-44 (Chem. Abs. 52, 1355a).

Novoselev, S. S. (1955) Effect of zinc sulfide on properties of copper mats. Tvetnye Metally. 28, no. 3, 15-20 (Chem. Abs. 54, 7476d).

Pankrantz, L. B., and King, E. G. (1970) High temperature enthalpies and entropies of chalcopyrite and bornite. U. S. Bureau of Mines Rept. Inv., 7435.

Panto, Gabor, and Panto, György (1972) Electron-probe check of Fe-distribution in sphalerite grains of the Nagybörysöny hydrothermal ore deposits, Hungary. Mineral. Deposita (Berl.), 7, 126-140.

Park, C. F. and MacDairmid, R. A. (1964) Ore deposits. W. H. Freeman and Company, San Francisco.

Pauly, Hans (1960) Paragenetic relations in the main cryolite ore of Ivigtut, South Greenland. Museum de Mineralogie it de Geologie de l'universite de Copenhague, Communications Geologigues, No. 106, 122-139.

Ridge, John D., ed. (1968) Ore deposits of the United States,1933-1967, The Graton-Sales Volume. New York, The American Institute of Mining, Metallurgical and Petroleum Engineers, Inc.

Roseboom, E. H. and Kullerud, G. (1958) The solidus in the system Cu-Fe-S between 400°C and 800°C. Carnegie Institute Wash. Yearbk., 57, 222-227.

Rucklidge, J. C. and Gasparrini, E. (1969) EMPADR VII--Specifications of a computer program for processing electron microprobe analytical data. Dept. Geol., Univ. Toronto.

Shannon, R. D., and Prewitt, C. T., (1969) Effective Ionic Radii in Oxides and Flourides. Acta Crystallographica, B25, Pt. 5, 925-946.

Sims, P. K., and Barton, P. B., Jr. (1961) Some aspects of the geochemistry of sphalerite, Central City District, Colorado. Econ. Geol., 56, 1211-1237.

Skinner, B. J., Barton, P. B., Jr., and Kullerud, G. (1959) Effect of FeS on the unit cell edge of sphalerite. Arevision. Econ. Geol., 54,1040-1046.

Stanton, R. L. (1972) Ore petrology. McGraw-Hill, Inc., New York.

Sugaki. A., Tashiro, C., and Hayashi, H. (1956) Skeletal crystals of sphalerite in chalcopyrite. Jour. Jap. Assoc. Min. Petr. Econ. Geol., 40, 12-21.

Toulmin, Priestly, III (1960) Effect of Cu on sphalerite phase equilibria, a preliminary report (abstract). Geol. Soc. America Bull. 71, 1933.

———— and Barton, P. B., Jr. (1964) A thermodynamic study of pyrite and pyrrhotite. Geochem. et Cosmochim. Acta., 28, 641-671.

Ulmer, Gene C. (ed.) (1971) Research techniques for high pressure and high temperature. Springer-Verlag, New York.

Uylenbogaardt, W. and Burke, E. A. J. (1971) Tables for microscopic identification of ore minerals. Elsevier Pub. Co., New York.

Winkler, H. G. F. (1967) Petrogenesis of metamorphic rocks. Springer-Verlag, New York.

Wright, J. B., and Lovering, J. F. (1967) Electron probe microanalysis and geothermometry of sphalerite in the Moke Creek Sulfide Sodo, Wakatipu, Queenstown. Amer. Min., 52, 524-529.

Yund, R. A. (1963) Crystal data for synthetic $Cu_{5-5x}Fe_xS_{6-5x}$ (idaite). Amer. Min., 48, 672-676.

———— and Kullerud, G. (1960) The Cu-Fe-S system. Carnegie Inst. Wash. Yearbk., 59, 111-114.

———————— (1961) The system Cu-Fe-S. Carnegie Inst. Wash. Yearbk., 60, 180-181.

———————— (1966) Thermal stabilities in the Cu-Fe-S system. Jour. Petrology, 7, 454-488.

APPENDIX I. EXPERIMENTAL DATA AND PRODUCTS

Run Number	Temp °C	Run Time # of Days	Starting Compositions in wt. % ZnS	CuS	FeS	FeS_2	Reaction Products[1]
1-A-1	800	30	20	20	60	--	po(Zn0,Cu.062,Fe.808,S);iss(Zn.2,Cu1.02,Fe1.8,S3)
1-A-2	800	30	20	40	40	--	sp(Zn.821,Cu.037,Fe.142,S);iss(Zn.283,Cu.795,Fe.923, S1.912)
1-A-3	800	30	20	60	20	--	sp(Zn.893,Cu.024,Fe.088,S);iss(Zn.32,Cu2.92,Fe1.56, S4);bn(Zn.12,Cu3.92,Fe1.41,S4)
1-A-4	800	30	40	40	20	--	sp(Zn.881,Cu.028,Fe.091,S);iss(Zn.32,Cu2.87,Fe1.62,S4)
1-A-5	800	30	60	20	20	--	sp(Zn.868,Cu.028,Fe.121,S);iss(Zn.22,Cu.94,Fe.84,S1.85)
1-A-6	800	30	40	20	40	--	sp(Zn.664,Cu.048,Fe.315,S);iss(Zn.21,Cu.82,Fe.96,S1.77)
1-A-7	800	30	33.3	33.3	33.3	--	sp(Zn.826,Cu.041,Fe.151,S);iss(Zn.28,Cu.82,Fe.89,S1.862)
1-B-1	700	30	20	20	60	--	po(Zn0,Cu.037,Fe.843,S);iss(Zn.147,Cu1.035,Fe1.862,S3); py(Zn.007,Cu0,Fe1.032,S2)
1-B-2	700	30	20	40	40	--	sp(Zn.835,Cu.074,Fe.167,S)[1];iss(Zn.18,Cu.83,Fe.98,S1.91)
1-B-3	700	30	20	60	20	--	sp(Zn.928,Cu.013,Fe.046,S);bn(Zn.09,Cu3.72,Fe1.43,S4); bn(Zn.09,Cu4.13,Fe1.26,S4)
1-B-4	700	30	40	40	20	--	sp(Zn.954,Cu.088,Fe.053,S);iss(Zn.20,Cu2.97,Fe1.59,S4)
1-B-6	700	30	40	20	40	--	sp(Zn.706,Cu.027,Fe.302,S);iss(Zn.13,Cu.90,Fe.97,S1.726)
1-B-7	700	30	33.3	33.3	33.3	--	sp(Zn.917,Cu.025,Fe.096,S);iss(Zn.18,Cu.87,Fe.96,S1.92)
1-C-1	600	30	20	20	60	--	sp(Zn.679,Cu.009,Fe.326,S);po(Zn0,Cu.009,Fe.326,S); iss(Zn.356,Cu.712,Fe1.935,S3)
1-C-2	600	30	20	40	40	--	sp(Zn.944,Cu.025,Fe.059,S);iss(Zn.15,Cu.91,Fe.94,S1.92); py
1-C-3	600	30	20	60	20	--	sp(Zn.909,Cu.072,Fe.043,S);py(Zn0,Cu0,Fe1.017,S2);bn (Zn.05,Cu4.4,Fe1.1,S4);iss
1-C-4	600	30	40	40	20	--	sp(Zn.921,Cu.075,Fe.045,S);py(Zn0,Cu0,Fe1.015,S2);bn (Zn.04,Cu4.58,Fe1.07,S4);iss
1-C-5	600	30	60	20	20	--	sp(Zn.985,Cu.005,Fe.03,S);iss(Zn.15,Cu.93,Fe.92,S1.92); py
1-C-6	600	30	40	20	40	--	sp(Zn.985,Cu.005,Fe.03,S);iss(Zn.286,Cu1.053,Fe1.77,S3)

1-C-7	700	30	33.3	33.3	33.3	--	sp(Zn.942,Cu.031,Fe.06,S);iss(An.22,Cu.89,Fe.89,S1.9); py
1-E-1	500	30	20	20	60	--	sp(Zn.692,Cu.003,Fe.316,S);po(Zn0,Cu.018,Fe.915,S); iss(Zn.155,Cu.785,Fe2.015,S3)[1]
1-E-2	500	30	20	40	40	--	sp(Zn.832,Cu.057,Fe.121,S);iss(Zn.304,Cu.815,Fe.881, S2.085)
1-E-3	500	30	20	60	20	--	sp(Zn.89,Cu.125,Fe.034,S);py(Zn.196,Cu.019,Fe.917,S2); bn(Zn.059,Cu4.781,Fe.88,S4);cp
1-E-4	500	30	40	40	20	--	sp(Zn.593,Cu.141,Fe.034,S);py(Zn.025,Cu.032,Fe.962,S2)[1]; iss(Zn.041,Cu3.338,Fe.647,S4)
1-E-5	500	30	60	20	20	--	sp(Zn.897,Cu.055,Fe.063,S);iss(Zn.353,Cu.791,Fe.857, S1.925)[1]
1-E-6	500	30	40	20	40	--	sp(Zn.876,Cu.002,Fe.209,S)[1];iss(Zn.119,Cu1.034,Fe1.903, S3)
1-E-7	500	30	33.3	33.3	33.3	--	sp(Zn.795),Cu.067,Fe.109,S);iss(Zn.254,Cu.844,Fe.901, S1.982);py
2-F-1	800	39	17	17	50	17	sp(Zn.684,Cu.062,Fe.288,S)[1];po(Zn0,Cu.051,Fe.824,S)[1]; iss(Zn.68,Cu.75,Fe1.6,S3)
2-F-2	800	39	17	33	33	17	iss(Zn.5,Cu.95,Fe1.6,S3)
2-F-3	800	39	17	50	17	17	sp(Zn.887,Cu.026,Fe.09,S);iss(An.34,Cu2.25,Fe1.65,S4)
2-F-4	800	39	33	33	17	17	sp(Zn.857,Cu.032,Fe.113,S);iss(Zn.25,Cu.83,Fe.92,S)
2-F-5	800	39	50	17	17	17	sp(Zn.766,Cu.041,Fe.181,S);iss(Zn.53,Cu.92,Fe1.5,S3)
2-F-6	800	39	33	17	33	17	sp(Zn.668,Cu.062,Fe.283,S);po(Zn0,Cu.037,Fe.829,S); iss(Zn.68,Cu.74,Fe1.53,S3)
2-F-7	800	39	27.8	27.8	27.8	17	sp(Zn.741,Cu.009,Fe.213,S);iss(Zn.57,Cu.88,Fe1.57,S3)
2-E-1	700	39	17	17	50	17	sp(Zn.746,Cu.02,Fe.203,S);iss(Zn.342,Cu.873,Fe1.756,S3); py(Zn0,Cu0,Fe1.023,S2);po
2-E-2	700	39	17	33	33	17	sp(Zn.82,Cu.016,Fe.118,S)[1];iss(Zn.283,Cu1.06,Fe1.585; S3)[1]
2-E-3	700	39	17	50	17	17	sp(Zn.792,Cu.181,Fe.05,S);iss(Zn.11,Cu1.09,Fe.79,S1.85)
2-E-4	700	39	33	33	17	17	sp(Zn.899,Cu.015,Fe.064,S);iss(Zn.17,Cu.87,Fe.96,S1.99)
2-E-5	700	39	50	17	17	17	sp(Zn.873,Cu.015,Fe.112,S);py(Zn.010,Cu0,Fe1.021,S2)[1]; iss
2-E-6	700	39	33	17	33	17	sp(Zn.79,Cu.021,Fe.197,S);iss(Zn.344,Cu.923,Fe1.744, S3);py(Zn0,Cu0,Fe1.027,S2)

2-E-7	700	39	27.8	27.8	27.8	17	sp(Zn.854,Cu.019,Fe.116,S);iss(Zn.308,Cu1.089,Fe1.606, S3)
2-D-1	600	39	17	17	50	17	sp(Zn.781,Cu.013,Fe.215,S);po(Zn0,Cu.017,Fe.874,S); iss(Zn.2,Cu.93,Fe1.89,S3)
2-D-2	600	39	17	33	33	17	sp(Zn.929,Cu.021,Fe.055,S);py(Zn0,Cu.001,Fe1.018,S2); iss(Zn.15,Cu.857,Fe.99,S1.98)
2-D-3	600	39	17	50	17	17	sp(Zn.971,Cu.01,Fe.027,S);iss(Zn.05,Cu1,Fe.85,S1.87)
2-D-4	600	39	33	33	17	17	sp(Zn.972,Cu.008,Fe.029,S);py(Zn0,Cu.013,Fe1.02,S2); iss(Zn.09,Cu1.,Fe.9,S1.94)
2-D-5	600	39	50	17	17	17	sp(Zn.972,Cu.013,Fe.043,S);py(Zn0,Cu0,Fe1.046,S2); iss(Zn.09,Cu.99,Fe.91,S1.91)
2-D-6	600	39	33	17	33	17	sp(Zn.895,Cu.005,Fe.131,S);iss(Zn.175,Cu.974,Fe1.882, S3)
2-D-7	600	39	27.8	27.8	27.8	17	sp(Zn.947,Cu.018,Fe.053,S);py(Zn0,Cu.0012,Fe1.038,S2); iss(Zn.08,Cu.91,Fe1.,S1.95)
2-B-1	500	39	17	17	50	17	py(Zn0,Cu0,Fe1.06,S2);sp(Zn.814,Cu.009,Fe.025,S); iss(Zn.294,Cu.953,Fe1.88,S3)
2-B-2	500	39	17	33	33	17	sp(Zn.888,Cu.063,Fe.081,S);py(Zn.015,Cu.034,Fe1.034,S2)
2-B-3	500	39	17	50	17	17	iss(Zn.124,Cu.910,Fe.965,S1.91)[1];py(Zn0,Cu.008,Fe1.046, S2);bn(Zn.04,Cu4.31,Fe1.07,S4)
2-B-4	500	39	33	33	17	17	sp(Zn.988,Cu.008,Fe.014,S);py(Zn.01,Cu.004,Fe1.041,S2);bn
2-B-5	500	39	50	17	17	17	sp(Zn.924,Cu.043,Fe.056,S);py(Zn0,Cu0,Fe1.045,S2); bn(Zn.03,Cu4.34,Fe1.04,S4)
2-B-6	500	39	33	17	33	17	iss(Zn.249,Cu1.025,Fe1.849,S3);py(Zn0,Cu0,Fe1.066,S2);sp
2-B-7	500	39	27.8	27.8	27.8	17	sp(Zn.923,Cu.039,Fe.069,S);iss(Zn.146,Cu.882,Fe.972, S1.93);py
3-A-20	800	30	5	5	90	--	sp(Zn.414,Cu.047,Fe.567,S);po(Zn0,Cu.033,Fe.958,S)
3-A-21	800	30	35	5	60	--	sp(Zn.374,Cu.047,Fe.605,S);po(Zn0,Cu.029,Fe.983,S)
3-A-22	800	30	25	25	50	--	sp(Zn.6,Cu.072,Fe.334,S);iss(Zn.693,Cu.712,Fe1.638,S3)
3-A-23	800	30	5	30	65	--	cb(Zn.142,Cu.911,Fe2.032,S3)
3-A-24	800	30	15	55	30	--	iss(Zn.25,Cu.87,Fe.88,S1.89);sp
3-A-26	800	30	5	80	15	--	sp(Zn.924,Cu.020,Fe.050,S)[1];bn(Zn.017,Cu4.09,Fe1.05,S4)
3-A-27	800	30	5	70	25	--	sp(Zn.882,Cu.04,Fe.09,S)[1];iss(Zn.26,Cu2.83,Fe1.60,S4)[1]; bn(Zn.14,Cu3.84,Fe1.23,S4)
3-A-28	800	30	70	10	20	--	sp(Zn.799,Cu.0413,Fe.172,S)[1];iss(Zn.3,Cu.78,Fe.92,S1.9)[1]

3-A-29	800	30	55	10	35	--	sp(Zn.551,Cu.075,Fe.401,S)[1];iss
3-A-30	800	30	45	10	45	--	sp(Zn.421,Cu.109,Fe.499,S)[1]
3-A-31	800	30	50	45	5	--	sp(Zn.423,Cu.117,Fe.479,S);po(Zn0,Cu.048,Fe.871,S)
		S.93	S.93	S.93			
3-A-32	800	30	30	63	34	--	iis(Zn.12,Cu2.9,Fe1.76,S4)
3-A-33	800	30	10	55	35	--	sp(Zn.867,Cu.062,Fe.120,S);iss(Zn.34,Cu2.49,Fe1.76,S4)
3-A-34	800	30	10	46	44	--	iss(Zn.162,Cu.99,Fe.85,S1.7);sp
3-A-35	800	30	10	40	50	--	iss(Zn.19,Cu.81,Fe1.,S1.81)
3-A-36	800	30	2	35	63	--	iss(Zn.076,Cu1.216,Fe2.061,S3)
		S.86	S.86	S.86			
3-A-37	800	30	3	63	34	--	iss(Zn.212,Cu1.381,Fe1.828,S3);bn(Zn.07,Cu3.89,Fe1.57, S4)
3-A-38	800	30	10	55	35	--	bn(Zn.02,Cu4.18,Fe1.43,S4),iss(Zn.14,Cu.88,Fe.98,S1.72); sp;cu
3-A-39	800	30	10	46	44	--	iss(Zn.16,Cu.95,Fe.89,S1.68)
3-A-40	800	30	10	40	50	--	bn(Zn.09,Cu3.75,Fe1.69,S4);Cu
3-A-41	800	30	2	35	63	--	iss(Zn.098,Cu1.50,Fe2.05,S3);po(Zn0,Cu.066,Fe.967,S); bn(Zn.02,Cu3.89,Fe1.61,S4);Fe(Zn.01,Cu0,Fe1.,S0);Cu
		S.93	S.93	S.93			
3-A-42	800	30	62	3	35	--	sp(Zn.657,Cu.019,Fe.356,S);iss;bn(Zn.14,Cu3.86,Fe1.5,S4)[1]
3-A-43	800	30	52	3	43	--	sp(Zn.552,Cu.024,Fe.462,S);Fe(Zn.01,Cu0,Fe1,S0); bn(Zn.0,Cu3.48,Fe1.87,S4)
3-A-44	800	30	37	3	60	--	sp(Zn.40,Cu.04,Fe.62,S);Cu;Fe
3-B-20	700	45	5	5	90	--	sp(Zn.305,Cu.087,Fe.668,S)[1];po(Zn0,Cu.031,Fe1.041,S)
3-B-22	700	45	25	25	50	--	sp(Zn.698,Cu.022,Fe.287,S)[1];iss(Zn.331,Cu.807,Fe1.987, S3)[1];po(Zn0,Cu.023,Fe.928,S)
3-B-23	700	45	5	30	65	--	iss(Zn.123,Cu.905,Fe2.141,S3)[1];po(Zn0,Cu.033,Fe.925,S)[1]
3-B-24	700	45	15	55	30	--	sp(Zn.944,Cu.014,Fe.05,S);iss(Zn.19,Cu2.93,Fe1.66,S4); bn(Zn.04,Cu5.02,Fe1.81,S4)[1]
3-B-25	700	45	5	65	30	--	sp(Zn.912,Cu.033,Fe.053,S);bn(Zn.03,Cu4.,Fe1.21,S4); iss(Zn.2,Cu2.83,Fe1.67,S4)
3-B-26	700	45	5	80	15	--	sp(Zn.978,Cu.027,Fe.021,S);bn(Zn.034,Cu4.684,Fe.919,S4)
3-B-27	700	45	5	70	25	--	sp(Zn.991,Cu.014,Fe.026,S);bn(Zn.06,Cu4.18,Fe1.22,S4); iss(Zn.15,Cu3.04,Fe1.7,S4)
3-B-28	700	45	70	10	20	--	sp(Zn.82,Cu.025,Fe.170,S);iss(Zn.36,Cu1.113,Fe1.731,S3)

3-B-29	700	45	55	10	35	--	sp(Zn.674,Cu.027,Fe.335,S);iss
3-B-30	700	45	45	10	45	--	sp(Zn.629,Cu.04,Fe.274,S)[1];iss(Zn.488,Cu.723,Fe1.937,S3); po(Zn0,Cu.03.Fe.901,S)
3-B-31	700	45	50	45	5	--	sp(Zn.728,Cu.03,Fe.269,S);iss(Zn.401,Cu.864,Fe1.84,S3); po(Zn0,Cu.034,Fe.854,S)
		S.93	S.93	S.93			
3-B-32	700	45	3	63	34	--	iss(Zn.24,Cu2.74,Fe1.74,S4);sp
3-B-33	700	45	10	55	35	--	iss(Zn.14,Cu2.91,Fe1.79,S4)
3-B-34	700	45	10	46	44	--	iss(Zn.16,Cu.83,Fe1.01,S1.83);sp
3-B-35	700	45	10	40	50	--	sp(Zn.756,Cu.035,Fe.236,S);iss(Zn.18,Cu.77,Fe1.05,S1.86)
3-B-36	700	45	2	35	63	--	iss(Zn.075,Cu1.039,Fe2.208,S3);sp
		S.86	S.86	S.86			
3-B-37	700	45	3	63	34	--	bn(Zn.06,Cu4.46,Fe1.34,S4);iss(Zn.123,Cu.84,Fe1.04,S1.76)[1]; Cu
3-B-38	700	45	10	55	35	--	sp(Zn.723,Cu.045,Fe.237,S);iss(Zn.09,Cu1.02,Fe.886,S1.692); bn(Zn.07,Cu4.3,Fe1.36,S4)
3-B-39	700	45	10	46	44	--	sp(Zn.707,Cu.040,Fe.279,S)[1];iss(Zn.1,Cu.92,Fe.98,S1.75)
3-B-40	700	45	10	40	50	--	iss;bn(Zn.06,Cu3.89,Fe1.5,S4);Cu
3-B-41	700	45	2	35	63	--	iss(Zn.03,Cu.95,Fe1.01,S1.8);Fe;sp
		S.93	S.93	S.93			
3-B-42	700	45	62	3	35	--	sp(Zn.613,Cu.005,Fe.396,S)[1];bn(Zn.1,Cu4.16;Fe1.41,S4)
3-B-43	700	45	52	3	43	--	sp(Zn.556,Cu.006,Fe.45,S)[1];Fe;Cu;bn
3-B-44	700	45	37	3	60	--	po(Zn0,Cu.017,Fe.991,S);iss(Zn.09,Cu3.156,Fe1.61,S4); Fe;Cu;bn
3-C-22	600	63	25	25	50	--	sp(Zn.762,Cu.017,Fe.237,S)[1];iss(Zn.388,Cu.905,Fe1.876,S3)
3-C-23	600	63	5	30	65	--	po(Zn0,Cu.021,Fe.875,S)[1];iss(Zn.149,Cu.908,Fe1.985,S3);sp
3-C-24	600	63	15	55	30	--	sp(Zn.927,Cu.034,Fe.056,S);iss(Zn.08,Cu1.02,Fe.9,S1.83)
3-C-25	600	63	5	65	30	--	sp(Zn.99,Cu.008,Fe.021,S)[1];iss(Zn.13,Cu2.67,Fe1.66,S4)
3-C-26	600	63	5	80	15	--	sp(Zn.955,Cu.012,Fe.047,S)[1];py(Zn0,Cu0,Fe1.02,S2)[1]; bn(Zn.06,Cu4.16,Fe.64,S4)[1];iss
3-C-27	600	63	5	70	25	--	sp(Zn.89,Cu.019,Fe.022,S);bn(Zn.09,Cu3.82,Fe1.09,S4);iss
3-C-28	600	63	70	10	20	--	sp(Zn.845,Cu.008,Fe.134,S);iss(Zn.205,Cu1.083,Fe1.731,S3)
3-C-29	600	63	55	10	35	--	sp(Zn.712,Cu.016,Fe.284,S);iss(Zn.187,Cu1.095,Fe1.852,S3)
3-C-30	600	63	45	10	45	--	sp(Zn.76,Cu.012,Fe.224,S);iss(Zn.247,Cu.889,Fe1.842,S3); po(Zn0,Cu0.2,Fe0.91,S)

3-C-31	600	63	50	45	5	--	sp(Zn.73,Cu.012,Fe.242,S);iss(Zn.219,Cu.868,Fe1.862,S3); po(Zn0,Cu.02,Fe.92,S)
			S.93	S.93	S.93		
3-C-32	600	63	3	63	34	--	sp(Zn.885,Cu.039,Fe.063,S);iss(Zn.15,Cu2.84,Fe1.7,S4)
3-C-33	600	63	10	55	35	--	sp(Zn.898,Cu.036,Fe.063,S);iss(Zn.14,Cu2.76,Fe1.72,S4)
3-C-34	600	63	10	46	44	--	iss(Zn.08,Cu.98,Fe.95,S1.8);sp
3-C-35	600	63	10	40	50	--	sp(Zn.777,Cu.017,Fe.197,S);iss(Zn.14,Cu.783,Fe1.11,S1.9)
3-C-36	600	63	2	35	63	--	iss(Zn.049,Cu1.037,Fe2.089,S3)
			S.86	S.86	S.86		
3-C-37	600	63	3	63	34	--	bn(Zn.03,Cu4.52,Fe1.12,S4);Cu
3-C-38	600	63	10	55	35	--	bn(Zn.108,Cu4.636,Fe1.188,S4);iss(Zn.07,Cu1.01,Fe.92, S1.76);sp;Cu
3-C-39	600	63	10	46	44	--	bn(Zn.093,Cu4.448,Fe1.335,S4);iss(Zn.08,Cu1.01,Fe.9, S1.69);sp;Cu
3-C-40	600	63	10	40	50	--	sp(Zn.405,Cu.045,Fe.571,S);iss(Zn.04,Cu1.,Fe.96,S1.69); bn(Zn.02,Cu3.78,Fe1.56,S4);Cu
3-C-41	600	63	2	35	63	--	iss(Zn.135,Cu1.146,Fe2.056,S3);iss(Zn.06,Cu3.32,Fe1.95, S4);Fe(Zn0,Cu0,Fe1.,S0);sp;Cu
			S.93	S.93	S.93		
3-C-42	600	63	62	3	35	--	sp(Zn.554,Cu.008,Fe.454,S);bn(Zn.05,Cu4.13,Fe1.4,S4); Fe;Cu
3-C-43	600	63	52	3	43	--	sp(Zn.558,Cu.005,Fe.464,S);Fe;Cu;bn
3-C-44	600	63	37	3	60	--	sp(Zn.433,Cu.012,Fe.573,S);po(Zn0,Cu.01,Fe1.014,S);Fe; Cu;bn
3-D-20	500	70	5	5	90	--	po(Zn0,Cu.022,Fe.967,S);sp
3-D-21	500	70	35	5	60	--	sp(Zn.9,Cu.025,Fe.098,S);iss(Zn.011,Cu.963,Fe1.025, S1.987);py(Zn0,Cu0,Fe1.019,S2)
3-D-22	500	70	25	25	50	--	sp(Zn.804,Cu.012,Fe.21,S);iss(Zn.128,Cu1.032,Fe1.893, S3)
3-D-23	500	70	5	30	65	--	iss(Zn.108,Cu.947,Fe2.049,S3);sp
3-D-24	500	70	15	55	30	--	sp(Zn.981,Cu.023,Fe.02,S);py(Zn0,Cu.022,Fe1.025,S3);bn
3-D-25	500	70	5	65	30	--	sp(Zn.97,Cu.026,Fe.018,S);bn(Zn.018,Cu4.446,Fe.920,S4); py(Zn0,Cu.029,Fe.999,S2)
3-D-26	500	70	5	80	15	--	sp(Zn.974,Cu.034,Fe.009,S);bn(Zn.039,Cu4.854,Fe.815, S4);py(Zn0,Cu.024,Fe1.016,S2)

3-D-27	500	70	5	70	25	--	sp(Zn.974,Cu.03,Fe.017,S);bn(Zn.035,Cu4.917,Fe.788,S4); py(Zn0,Cu.014,Fe1.006,S2);id(Zn.02,Cu3.11,Fe.65,S4)
3-D-28	500	70	70	10	20	--	sp(Zn.903,Cu.006,Fe.108,S);iss(Zn.067,Cu.817,Fe1.116, S1.918)
3-D-29	500	70	55	10	35	--	sp(Zn.770,Cu.005,Fe.25,S);iss(Zn.112,Cu1.15,Fe1.95,S3)
3-D-30	500	70	45	10	45	--	sp(Zn.832,Cu.004,Fe.197,S);iss(Zn.146,Cu.97,Fe1.99,S3); py(Zn0,Cu0,Fe1.025,S2);po(Zn0,Cu0.01,Fe.91,S)
3-D-31	500	70	50	45	5	--	sp(Zn.721,Cu.004,Fe.298,S);iss(Zn.129,Cu.856,Fe2.143,S3); py
			S.93	S.93	S.93		
3-D-32	50	70	3	63	34	--	iss(Zn.077,Cu3.046,Fe1.747,S4);bn
3-D-33	500	70	10	55	35	--	sp(Zn.96,Cu.047,Fe.06,S);iss(Zn.11,Cu2.43,Fe1.93,S4)
3-D-34	500	70	10	46	44	--	sp(Zn.861,Cu.026,Fe.13,S);iss(Zn.052,Cu.927,Fe1.022,S1.838)
3-D-35	500	70	10	40	50	--	sp(Zn.812,Cu.019,Fe.20,S);iss(Zn.06,Cu.812,Fe1.128,S1.842)
3-D-36	500	70	2	35	63	--	iss(Zn.051,Cu1.01,Fe2.10,S3);sp
			S.86	S.86	S.86		
3-D-37	500	70	3	63	34	--	bn(Zn.021,Cu5.056,Fe1.196,S4);bn(Zn.0,Cu3.89,Fe1.389,S4)
3-D-38	500	70	10	55	35	--	bn(Zn.01,Cu4.897,Fe1.166,S4);iss(Zn.04,Cu.99,Fe.96,S1.69); sp
3-D-39	500	70	10	46	44	--	sp(Zn.765,Cu.032,Fe.235,S);bn(Zn.015,Cu5.066,Fe1.179,S4); iss(Zn.04,Cu.94,Fe1.01,S1.74)
3-D-40	500	70	10	40	50	--	sp(Zn.477,Cu.028,Fe.509,S);iss(Zn.089,Cu1.12,Fe2.079,S3); bn(Zn.035,Cu4.74,Fe1.244,S4)
3-D-41	500	70	2	35	63	--	iss(Zn.104,Cu1.175,Fe2.083,S3);bn(Zn.03,Cu4.37,Fe1.44, S4);sp
			S.93	S.93	S.93		
3-D-42	500	70	62	3	35	--	sp(Zn.816,Cu.002,Fe.224,S);Cu(Zn.27,Cu1,Fe0,S0)
3-D-43	500	70	52	3	43	--	sp(Zn.554,Cu.003,Fe.473,S);bn(Zn.041,Cu5.222,Fe1.263,S4)[1]; Fe(Zn0,Cu0,Fe1,S0);Cu
3-D-44	500	70	37	3	60	--	sp(Zn.512,Cu.002,Fe.514,S);po(Zn0,Cu.005,Fe1.019,S)

[1]Designation for microprobe analyses which total between 104 to 102 and 98 to 96 unnormalized weight percent. All other totals are within the range 102 to 98 unnormalized weight percent.

APPENDIX II

Experimental Results of Sphalerite Unit Cell Determinations

Run Number	Analysis in Mole Percent			In Å	
	ZnS	CuS	FeS	a_o obs	a_o calc
A-20	39.64	4.61	55.75	5.4123	5.4279
A-22	59.71	7.11	33.18	5.4121	5.4234
A-26	92.96	1.99	5.05	5.4027	5.4120
A-28	79.02	4.06	16.93	5.4081	5.4176
B-26	95.35	2.58	2.07	5.4120	5.4104
B-27	96.37	1.21	2.42	5.4129	5.4106
B-28	80.83	2.41	16.77	5.4102	5.4186
B-29	65.20	2.50	32.30	5.4134	5.4232
B-30	60.32	3.80	35.88	5.4117	5.4242
B-31	71.00	2.82	26.18	5.4110	5.4212
C-33	90.23	3.51	6.25	5.4120	5.4126
E-4	92.14	1.38	6.48	5.4104	5.4127

APPENDIX III

Data Obtained from Analysis of Pyrrhotite Indicators

Sample Number	Pyrrhotite $\bar{1}01\bar{2}$ peak	D	N_{FeS}	log f_{S_2}	log α_{FeS}
		A Series	800°C		
21	43.3450	2.0874	.9880	-6.2803	-3.3712
22	43.9450	2.0603	.9369	-1.1936	-8.5339
23	43.8575	2.0642	.9442	-1.7348	-7.9652
24			**		
25			**		
26			**		
27			**		
28			**		
29	43.6300	2.0744	.9635	-3.3600	-6.2882
30	43.7250	2.0701	.9555	-2.6356	-7.0302
31	43.9690	2.0592	.9349	-1.0514	-8.6843
32			**		
33			**		
34	43.8825	2.0631	.9421	-1.5763	-8.1312
35	43.7790	2.0677	.9509	-2.2551	-7.4235
36	43.5330	2.0788	.9718	-4.1932	-5.4445
37	43.5290	2.0790	.9722	-4.2301	-5.4073
38	43.6155	2.0751	.9648	-3.4778	-6.1683
39	43.6350	2.0742	.9631	-3.3198	-6.3291
40	43.3900	2.0853	.9841	-5.6953	-3.9471
41	43.2975	2.0896	.9921	-7.0014	-2.6662
42			*		
43			*		
44			*		
		B Series	700°C		
22	44.1650	2.0505	.9185	-0.8168	-9.8377
23	43.9383	2.0606	.9374	-2.2327	-8.4917
24			**		
25			**		
26			**		
27			**		
28	44.2170	2.0482	.9142	-0.5167	-10.1246
29	43.7550	2.0688	.9529	-3.5430	-7.2509
30	44.0660	2.0549	.9267	-1.4119	-9.2705
31	44.1932	2.0493	.9161	-0.6531	-9.9941
32			**		
33			**		
34	43.8530	2.0644	.9446	-2.8219	-7.9350
35	43.7405	2.0694	.9541	-3.6607	-7.1450

36	43.5105	2.0798	.9737	-5.7015	-5.2327
37	43.5740	2.0769	.9683	-5.0802	-5.8137
39	43.6260	2.0746	.9639	-4.6087	-6.2553
40	43.3560	2.0869	.9870	-7.5188	-3.5188
41			*		
42			*		
43			*		
44			*		
		C Series	600°C		
21	44.0110	2.0573	.9313	-2.9239	-8.9422
22	43.5102	2.0798	.9738	-7.2996	-5.2298
23	44.0037	2.0576	.9319	-2.9765	-8.8981
24	44.0560	2.0553	.9276	-2.6023	-9.2116
25			**		
26			**		
27			**		
28	44.1786	2.0499	.9174	-1.7628	-9.9134
29	43.6134	2.0752	.9649	-6.2261	-6.1508
30	44.1785	2.0499	.9174	-1.7634	-9.9128
31	44.0483	2.5571	.9282	-2.6565	-9.1661
32	44.0835	2.0541	.9253	-2.4095	-9.3729
33	44.1776	2.0500	.9174	-1.7690	-9.9082
34	43.6710	2.0726	.9600	-5.6791	-6.6171
35	43.7100	2.0708	.9567	-5.3560	-6.9176
36	43.5100	2.0798	.9738	-7.3019	-5.2279
37	43.5303	2.0789	.9720	-7.0790	-5.4197
38	43.6450	2.0737	.9623	-5.9221	-6.4102
39	43.6050	2.0755	.9657	-6.3087	-6.0803
40	43.3154	2.0887	.9906	-9.9140	-2.9467
41	43.3155	2.0887	.9905	-9.9123	-2.9482
42			*		
43	43.2200	2.0931	.9988	-12.0304	-1.0448
		D Series	500°C		
21			*		
22	43.5983	2.0758	.9662	-8.2865	-6.0238
23	43.5940	2.0760	.9666	-8.3344	-5.9868
24	43.9850	2.0585	.9335	-4.6093	-8.7833
25	44.0063	2.0575	.9317	-4.4309	-8.9138
26	44.0065	2.0575	.9317	-4.4295	-8.9148
27	43.9590	2.0596	.9357	-4.8293	-8.6219
28	43.9450	2.0603	.9369	-4.9491	-8.5339
29	43.5650	2.0773	.9691	-8.6607	-5.7344
30	44.0660	2.0549	.9267	-3.9395	-9.2720
31	43.9940	2.0581	.9328	-4.5338	-8.8386
32	44.0280	2.0566	.9299	-4.2516	-9.0447
33	43.9940	2.0581	.9328	-4.5338	-8.8386

34	43.6070	2.0754	.9655	-8.1914	-6.0971
35	43.6150	2.0751	.9648	-8.1042	-6.1641
36	43.3916	2.0852	.9840	-10.8918	-3.9671
37	43.4080	2.0845	.9826	-10.6537	-4.1594
38	43.3250	2.0883	.9897	-11.9635	-3.0892
39	43.5775	2.0768	.9680	-8.5188	-5.8443
40	43.2945	2.0897	.9924	-12,5293	-2.6170
41	43.3356	2.0878	.9888	-11.7789	-3.2420
42	43.2175	2.0932	.9990	-14.4410	-0.9702
43	43.2270	2.0928	.9982	-14.1342	-1.2403
44	43.2096	2.0936	.9997	-14.7278	-0.7156

---

* Pyrrhotite peak broadened powder diffraction tracing indicates high percentage of iron.

** Sulfur solidified on quench.

APPENDIX IV

Microprobe Analyses of Natural Sphalerite Chalcopyrite Assemblages

Sample Number and Location		Analyses[1]
20	Eagle Mine, Oklahoma	Cp(ZnS0.0,CuS49.6,FeS50.4); Sp(ZnS99.6,CuS0.0,FeS0.4)
51	Osborne Lake Mine, Manitoba	Cp(ZnS0.71,CuS49.59,FeS49.69); Sp(ZnS90.33,CuS0.2,FeS9.47); Po(ZnS0.44,CuS0.0,FeS99.56); Py(ZnS0.04,CuS0.0,FeS99.96)
52	Flexar Lake Mine, Manitoba	Cp(ZnS0.82,CuS48.74,FeS50.44); Sp(ZnS89.63,CuS0.6,FeS9.76); Po(ZnS0.2,CuS0.58,FeS99.22)
55	Ghost Lake Mine, Manitoba	Cp(ZnS0.17,CuS48.88,FeS50.95); Sp(ZnS84.99,CuS0.0,FeS15.0); Po(ZnS0.0,CuS0.0,FeS100.0)
58	Stahl Lake Mine, Manitoba	Cp(ZnS0.0,CuS49.11,FeS50.89); Sp(ZnS89.77,CuS0.18,FeS10.04); Po(ZnS0.0,CuS0.0,FeS100.0); Py(ZnS0.0,CuS0.0,FeS100.0)
59	Chisel Lake Mine, Manitoba	Cp(ZnS0.0,CuS47.86,FeS52.14); Sp(ZnS84.2,CuS0.0,FeS15.8); Po(ZnS0.0,CuS0.0,FeS100.0); Py(ZnS0.0,CuS0.0,FeS100.0)
60	White Lake Mine, Manitoba	Cp(ZnS0.23,CuS48.59,FeS51.17); Sp(ZnS84.46,CuS0.05,FeS15.49); Po(ZnS1.02,CuS0.0,FeS98.98)
62	Dickstone Mine, Ontario	Cp(ZnS0.48,CuS48.52,FeS51.0); Sp(ZnS86.65,CuS0.44,FeS12.9); Po(ZnS0.0,CuS0.0,FeS100.0)
78	Fox Lake Mine, Manitoba	Cp(ZnS0.39,CuS48.46,FeS51.14); Sp(ZnS84.54,CuS0.0,FeS15.46); Po(ZnS0.0,CuS0.0,FeS100.0); Cb(ZnS0.0,CuS33.46,FeS66.54)
80	Fox Lake Mine, Manitoba	Cp(ZnS0.0,CuS48.25,FeS51.74); Sp(ZnS82.2,CuS0.0,FeS17.79); Po(ZnS0.0,CuS0.0,FeS100.0)
83	Ruttan Mine, Manitoba	Cp(ZnS0.0,CuS48.75,FeS51.25); Sp(Zn88.67;CuS0.27,FeS11.06); Po(ZnS0.21,CuS0.0,FeS99.79); Py(ZnS0.0,CuS0.0,FeS100.0)

84	Ruttan Mine, Manitoba	Cp(ZnS0.0,CuS48.91,FeS51.08); Sp(ZnS84.78,CuS0.0,FeS15.22); Po(ZnS0.0,CuS0.0,FeS100.0); Py(ZnS0.0,CuS0.0,FeS100.0); Cb(ZnS0.0,CuS31.8,FeS68.2)
85	Ruttan Mine, Manitoba	Cp(ZnS0.38,CuS48.46,FeS51.15)[1]; Sp(ZnS83.77,CuS0.05,FeS16.18); Po(ZnS0.0,CuS0.0,FeS100.0); Cb(ZnS0.41,CuS32.77,FeS66.82)[1]
88	Fox Mine, Manitoba	Cp(ZnS1.37,CuS48.42,FeS50.2)[1]; Sp(ZnS85.77,CuS0.03,FeS14.2); Po(ZnS1.05,CuS0.0,FeS98.94); Py(ZnS0.0,CuS0.0,FeS100.0); Cb(ZnS0.0,CuS33.93,FeS66.93)
91	Fox Mine, Manitoba	Cp(ZnS2.45,CuS48.01,FeS49.53); Sp(ZnS86.47,CuS0.19,FeS13.34)[1]; Po(ZnS1.02,CuS0.0,FeS98.97)
524	Gossan Lead, Virginia	Cp(ZnS0.18,CuS48.59,FeS51.22)[1]; Sp(ZnS98.8,CuS0.41,FeS0.78); Po(ZnS0.0,CuS0.0,FeS100.0); Py(ZnS0.0,CuS0.0,FeS100.0)

VITA

Lovell B. Wiggins was born September 7, 1946 in Charlottesville, Virginia. He received a B.A. in biology from the University of Virginia, Charlottesville, Virginia in June 1968. Following a four year tour of duty in the USAF, he entered VPI and SU as a candidate for the M.S. in geological science.

L.B. Wiggins

A RECONNAISSANCE INVESTIGATION OF CHALCOPYRITE-SPHALERITE RELATIONSHIPS IN THE Cu-Fe-Zn-S SYSTEM

by

Lovell B. Wiggins

(ABSTRACT)

Reconnaissance investigation of the Cu-Fe-Zn-S system has been conducted into the phase equilibria of the geologically significant portion containing pyrrhotite, pyrite, bornite, chalcopyrite, cubanite, and sphalerite. Chalcopyrite-sphalerite relationships were emphasized because of their common association as intimately intergrown phases (interpreted as exsolution or replacement) in major Cu-Zn ore bodies. The investigation employed silica tube-type experiments in the temperature range 800°C to 500°C. Data indicate that solid solubility of ZnS in intermediate solid solution (a high temperature chalcopyrite-like phase) and of CuS and FeS in sphalerite depend on temperature, sulfur content, and metal:metal ratios. Illustrations of temperature and sulfur controls are listed below:

CuS in sphalerite - temperature - 800°C, 11.74 mole percent
500°C, 3.36 mole percent
sulfur content - excess - 800°C, decreases from 11.74 to 6.03
deficiency - 800°C, decreases from 11.74 to 5.98

ZnS in iss - temperature - 800°C, 22.73 mole percent
500°C, 4.67 mole percent
sulfur content - excess - 800°C, decreases from 22.73 to 7.1 (with Fe)

Variation of Cu/Fe ratios in iss from 23.93/53.88 to 40.51/50.08 produces a change of ZnS solubility in iss from 22.73 mole percent to 9.4 mole percent. It is concluded that intergrowths found in ores may

result from reduction in temperature, change in sulfur activity or ordering in a crystal structure. The low levels of impurity found in natural sphalerites and chalcopyrites indicate their virtual total expulsion on cooling.